Wave scattering by an infinite cascade of non-overlapping blades

Georg Maierhofer[a,*], N. Peake[a]

[a]*Department of Applied Mathematics and Theoretical Physics, University of Cambridge, UK*

Abstract

We consider the scattering of waves by an infinite three-dimensional cascade of finite-length flat blades in subsonic flow at zero angle of attack. This geometry is of specific relevance as it provides a model for the components in turbofan engines. We study the scattering problem analytically, considering both acoustical and vortical incident fields, spanwise wavenumbers and transverse mean flow. Most importantly we extend previous work by lifting the restriction that adjacent blades overlap, a condition that had thus far been crucial for the analytical study of this problem. Our method of solution relies on the solution of three coupled boundary value problems using the Wiener-Hopf technique, corresponding to an uncoupled leading-edge approximation, and a subsequent trailing-edge and leading-edge correction. We provide exact expressions for observables in the system, depending only on the solution of a linear matrix equation. Specifically we find closed-form expressions for the far-field behaviour of the scattered potential upstream and downstream of the cascade, the upstream and downstream sound power, as well as the total unsteady lift on each blade in the cascade. A wide range of results are presented, and we see that the non-overlapping cascade is, as might be expected, typically more transparent to incident disturbances than the previously studied overlapping case.

Keywords: Acoustic scattering, Wiener-Hopf method, Periodic structures, Acoustic interactions

1. Introduction

Understanding noise generation and propagation in modern aircraft engines is of crucial importance to help control noise emissions. In this paper we are concerned with the scattering of sound and vorticity waves by a cascade of finite length blades in mean-flow, which provides a model for the rotor and stator stages in turbofan engines. In modern turbomachinery the noise emission from the fan is one of the most dominant contributions to the total noise [1], and

*Corresponding author
Email address: g.maierhofer@maths.cam.ac.uk (Georg Maierhofer)

moreover the 'blockage' of sound generated elsewhere by the fan is a key element in any prediction of far-field noise. Consequently insights into the acoustic processes involved in scattering by a blade row are particularly relevant.

The scattering problem by a cascade of blades has been subject to a large amount of research over the past decades. The groundwork for the analytical solution of these types of problems was laid in a sequence of works by Carlson and Heins [2], Heins and Carlson [3] and Heins [4], who considered an analogous problem of electromagnetic scattering by a cascade of perfectly conducting semi-infinite blades extending to $x = +\infty$. One of the earliest works considering a cascade of finite-length blades was presented by Kaji and Okazaki [5], who considered a sound wave incident on the cascade and developed a numerical scheme based on a distribution of doublets to match the pressure jump on the blades. The problem was further studied by Whitehead [6] who developed the LINSUB code which provides a numerical scheme to solve for a variety of incident fields on a cascade located in subsonic mean-flow. This approximate solution is based on expanding the full pressure field in terms of separable waves in the Prandtl-Glauert plane and using a collocation type approach to match the upwash velocity at the blades. A more analytically-based approach was given by Koch [7], who used a scalar Wiener-Hopf formulation (of similar nature to [2]) to solve the problem of incident sound waves exactly (up to the truncation of an infinite system of linear equations) in the case of overlapping blades, thus allowing the computation of the scattered radiation in this case.

More recent work has focused on extending these results to incorporate more general geometries and incident fields, as well as to allow for a more efficient, and hence practically feasible solution. Peake [8] derived an asymptotic kernel factorisation for the large reduced frequency regime and used a small number of iterates in a Schwarzschild-type approach to produce an efficient scheme for an incident vorticity wave, which allows for the computation of the unsteady lift distribution. This asymptotic kernel factorisation was later extended by Peake and Kerschen [9] to be uniformly valid even for close to cut-off conditions of the radiation modes or duct modes. A subsequent work by Peake [10] solves the complete system exactly using a Wiener-Hopf type approach and presents an expression for the unsteady lift distribution that is valid for arbitrary reduced frequency. In both cases the method of solution relies on an assumption of overlap of adjacent blades in order to arrive at a coupling of the Wiener-Hopf equations that describe the leading-edge and trailing-edge interaction problems. Glegg [11] further extended the analysis to blades in a three-dimensional setting, including the effects of spanwise wave number and cross-flow, and analysed in detail the unsteady loading and far-field behaviour of the scattered field for an incident vortical gust. Glegg's method of solution can be motivated by a Schwarzschild-type distribution of boundary conditions, and results in a system of four coupled scalar Wiener-Hopf equations, which takes an essentially similar form to the one derived by [10]. These can then be solved, and an exact expression for the solution can be found which relies only on the solution of a linear matrix equation.

In recent years several studies have succeeded in analysing the effect of re-

alistic blade geometry, periodicity and mean flow on the cascade scattering problem. In particular Peake and Kerschen [12, 13] studied the effect of blade mean loading on the generation of noise in the case of mean flow that is aligned at a non-zero incidence angle to the cascade blades. The analytical studies of the cascade also provided a basis for Posson et al. [14], who were able to use the two-dimensional cascade solution as a source distribution for the scattering problem on an annular blade-row. Ayton and Peake [15] used the same velocity potential and streamfunction coordinate system as had been applied in [12, 13] to analyse realistic airfoil shapes by reduction to flat blades and appropriate boundary conditions. This coordinate system was successfully used by Baddoo and Ayton [16] to find an exact solution to the scattering problem by an infinite cascade of airfoils again based on the solution presented in [11].

However, in all of the aforementioned work, which uses the Wiener-Hopf technique to find either exact or approximate solutions to the scattering problem, the restriction to the case of overlapping blades is required. This restriction was necessary in previous studies because it effectively allows the Wiener-Hopf analysis to be based on the duct modes, which are the only modes present in overlapping parts of the geometry. If the blades do not overlap the modal structure is more complicated and the Wiener-Hopf solution needs to account for that. The main novelty of this paper is to present the first analytical solution which does not rely on overlapping blades and is in fact valid for arbitrary blade spacing. This is achieved by a formulation as a system of coupled scalar Wiener-Hopf equations, and by judiciously choosing an appropriate additive Wiener-Hopf splitting (which is described in detail in §4.3), that allows us to reduce the scattering problem to an infinite system of linear equations. Our additive splitting is based on the radiation modes, which leads to a discrete linear system with decaying coefficients that can be solved by truncation regardless of the choice of overlap. In contrast, the coefficients of the linear systems in previous work would increase exponentially when the blades do not overlap, so do not provide a convergent method in this case. We derive our solution in a very general three-dimensional setting, allowing for effects of spanwise wave number and cross-flow, as well as considering both incident vorticity and acoustic waves. This solution allows us to derive exact expressions for the far-field radiation and the unsteady lift on the blades, which, similarly to the previous work, are in closed form apart from the need to solve the aforementioned linear system numerically.

We begin this paper by outlining the equations of motion together with the relevant boundary conditions in §2. This is followed by a formulation of the scattering problem as a system of coupled Wiener-Hopf equations in §3, which is then solved using a Cauchy-type additive splitting in §4. The solution can be reduced to an infinite system of linear equations and this reduction is described in §5. It is possible to derive expressions for the total unsteady lift and the far-field sound based on our solution to the scattering problem, and these expressions are provided in §6. Finally, we provide numerical results using our solution in §7 which are used to demonstrate the accuracy of our method based on previous work in the overlapping case and to study the effects of

cascade geometry and spanwise wavenumber on the scattered field. Our results are summarised and an outlook of possible future research is provided in the concluding remarks in §8.

2. The equations of motion and mathematical formulation

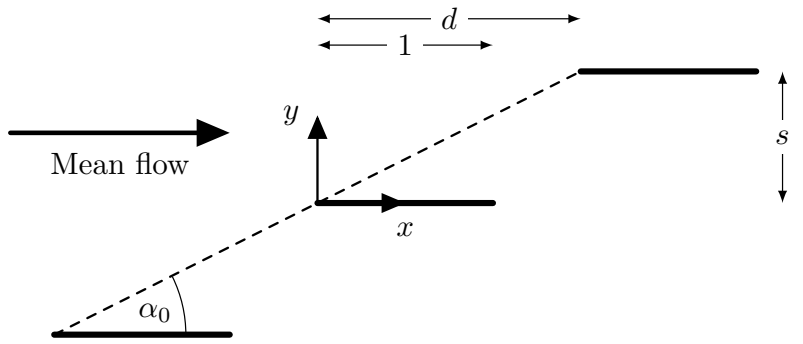

(a) Projection onto the xy-plane.

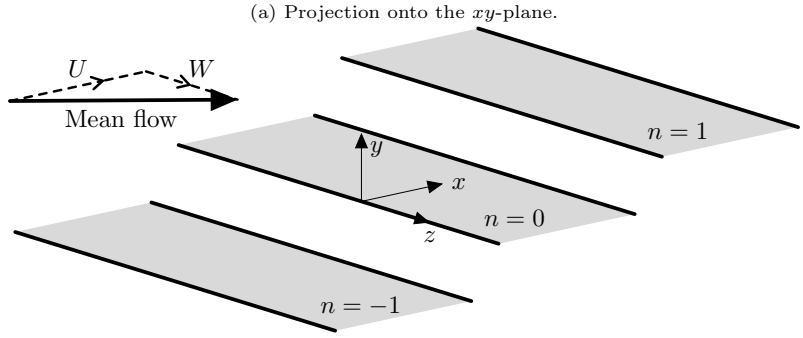

(b) Full three-dimensional geometry.

Figure 1: The cascade geometry with mean-flow and blade labels.

We consider a cascade of blades of zero thickness and camber, which are parallel to the xz-plane, of finite length in the x-direction, staggered in the y-direction and extend to infinity in the spanwise z-direction as shown in figure 1. We assume the blades lie in non-zero uniform subsonic mean flow $\mathbf{u} = (U, 0, W)$, with corresponding speed $U_\infty := \sqrt{U^2 + W^2}$ and Mach number $M := U_\infty/c_0$, with c_0 the undisturbed speed of sound. We suppose that the flow is perturbed by an incoming wave (which could correspond to an acoustic wave or a vortical gust) that is incident from $x = -\infty$. Then by Goldstein's splitting theorem [17, pp. 220-222] the perturbed velocity potential can be decomposed into a solenoidal part (which is zero for incident acoustic waves, and equal to the incident field for vorticity waves) and an irrotational part corresponding to the scattered field (plus the incident field for acoustic waves). The scattered

component $\tilde{\phi}(x, y, z, t)$ of this velocity potential satisfies

$$\frac{1}{c_0^2}\frac{\mathrm{D}^2\tilde{\phi}}{\mathrm{D}t^2} - \nabla^2\tilde{\phi} = 0, \tag{1}$$

where ∇^2 is the Laplacian in three dimensions. We non-dimensionalise our equations by rescaling the physical quantities as follows: We rescale lengths by l the blade chord, times by l/U_∞, density perturbations by the undisturbed fluid density ρ_0, pressure fluctuations by $\rho_0 U_\infty^2$, and we let $M_x := U/c_0, M_z := W/c_0$ be Mach numbers of the x, z-components of the flow. Finally the normalised blade stagger d, and interblade spacing s are defined as in figure 1a, resulting in the stagger angle $\alpha_0 = \arctan(s/d)$. Crucially, we wish to include the case of non-overlapping blades, so that d may be greater than 1.

We look for wave-like solutions of the form:

$$\tilde{\phi}(\mathbf{x}, t) = \phi(x, y)e^{i\Omega t - iK_3 z},$$

where $\Omega = \omega l/U_\infty$ is the reduced frequency, and $K_3 = lk_3$ is the non-dimensional spanwise wave number. Then, by Eq. (1), ϕ must satisfy the dimensionless equation

$$\beta^2\partial_x^2\phi + \partial_y^2\phi - 2i\tilde{\Omega}M_x M\partial_x\phi + \left(\tilde{\Omega}^2M^2 - K_3^2\right)\phi = 0, \tag{2}$$

where we denoted the Prandtl-Glauert number by $\beta^2 = 1 - M_x^2$, and we call $\tilde{\Omega} = \Omega - K_3\frac{M_z}{M}$ the effective reduced frequency, where we require $\tilde{\Omega}^2M_x^2 \geq K_3^2\beta^2$ for propagating acoustic modes to exist (as will be seen from the dispersion relation Eq. (5)).

2.1. Boundary conditions

Let us label the blades by $0, \pm1, \pm2, \ldots$, then for incident harmonic waves (either vortical or acoustical) the (time-dependent) upwash normal to the n^{th} blade (the y-velocity of the incoming wave on the blades in the upward pointing direction) is given by

$$V_g \exp\left(i\Omega t - iK_1 x + in\sigma\right), \tag{3}$$

where $K_1 = lk_1$ is the non-dimensional x-component of the wavevector, and we assume that the incident wave is periodic in the transverse direction, with the change in its phase between adjacent blades (the so-called interblade phase angle) being $\sigma = -dK_1 - sK_2$. In summary, ϕ must therefore satisfy the following conditions:

(i) The total normal velocity (i.e. the sum of upwash and normal component of the scattered potential) must vanish on the rigid stationary blades, i.e.

$$\frac{\partial\phi}{\partial y} = -V_g e^{in\sigma - iK_1 x} \text{ on } \{0 \leq x - nd \leq 1, y = ns\}.$$

(ii) The unsteady pressure, which is given in dimensionless form by

$$p = -\frac{\mathrm{D}\tilde{\phi}}{\mathrm{D}t} = -\left(i\tilde{\Omega}\frac{M}{M_x} + \frac{\partial}{\partial x}\right)\phi,$$

is continuous away from the blades. Note we have rescaled the pressure by a factor of M_x/M for ease of notation in the later Wiener-Hopf analysis where this would appear as a constant factor in the multiplicative kernel.

(iii) The scattered field must satisfy a radiation condition, which, with our introduction of the small fictitious damping $\mathrm{Im}\,\Omega < 0$ is equivalent to requiring ϕ to be bounded at infinity.

(iv) The incident field has a periodicity as specified in Eq. (3). We require the scattered potential to exhibit a similar property, namely for all $-\infty < x < \infty, 0 \le y \le s$:

$$\phi(x, y) = e^{-in\sigma}\phi(x + nd, y + ns). \tag{4}$$

This means in particular that we need only determine the velocity potential in the first cascade strip $\{-\infty < x < \infty, 0 \le y \le s\}$, and the solution everywhere else is determined from Eq. (4).

(v) The total velocity normal to the blades $\frac{\partial \phi}{\partial y}$ must be continuous everywhere (which follows from the continuity of pressure and the consideration of infinitely thin blades).

(vi) The scattered field satisfies the Kutta condition at the trailing edge (see for instance [8, 18]), i.e. $[p]$ is non-singular at the points $(x, y) = (1 + nd, ns)$, and the usual inverse square-root singularity at the leading edge, i.e. ϕ has an inverse square-root singularity at the points $(x, y) = (nd, ns)$.

In the present work we are particularly interested in incident (harmonic) vortical gusts and acoustic waves, as follows.

Incident harmonic gust

A harmonic vortical disturbance, representing for instance a component of the wake shed from an upstream blade row, corresponds to an incident velocity field of the form

$$\mathbf{u}_{inc} = \mathbf{A}e^{i\Omega t - i\mathbf{K}\cdot\mathbf{x}},$$

which must satisfy mass conservation $\nabla \cdot \mathbf{u}_{inc} = 0$, i.e. $\mathbf{A} \cdot \mathbf{K} = 0$, and is convected with the flow, i.e.

$$\frac{\mathrm{D}}{\mathrm{D}t}\mathbf{u}_{inc} = 0.$$

This results in the dispersion relation

$$K_1 = \tilde{\Omega} M M_x^{-1},$$

and implies $\sigma = -d\tilde{\Omega}MM_x^{-1} - sK_2$.

Incident acoustic waves

Acoustic waves, representing perhaps noise generated elsewhere in the aero-engine, have a velocity potential proportional to

$$e^{i\Omega t - iK_1 x - iK_2 y - iK_3 z},$$

which satisfies the convected wave equation Eq. (1). Thus we find the following dispersion relation

$$\beta^2 \left(K_1 + \frac{\tilde{\Omega} M_x M}{\beta^2} \right)^2 + K_2^2 + K_3^2 = \frac{\tilde{\Omega}^2 M^2}{\beta^2}. \tag{5}$$

This ellipsoid in wave phase space can be parametrised as follows:

$$K_1 = \frac{\tilde{\Omega} M \cos\varphi \sin\theta}{1 + M_x \cos\varphi \sin\theta}, \tag{6}$$

$$K_2 = \frac{\tilde{\Omega} M \sin\varphi \sin\theta}{1 + M_x \cos\varphi \sin\theta}, \tag{7}$$

$$K_3 = \frac{\tilde{\Omega} M \cos\theta}{1 + M_x \cos\varphi \sin\theta}. \tag{8}$$

From this parametrisation we can immediately extract the incident direction of the wave (in terms of azimuthal angle φ and polar angle θ). Moreover, in terms of φ, θ we have

$$\sigma = \frac{(-\sin\theta)\tilde{\Omega} M}{1 + M_x \cos\varphi \sin\theta} \left(d\cos\varphi + s\sin\varphi \right).$$

Although our methodology can easily be extended to the case of incident acoustic waves from downstream, we focus in this paper on the case of upstream incidence, which for us means $s(M_x + \sin\theta\cos\varphi) - d\sin\theta\sin\varphi \geq 0$ and is specified in more detail in §3.1.

3. Formulation as a Wiener-Hopf problem

The periodicity condition (iv) allows us to restrict ourselves to the first cascade strip $\{-\infty < x < \infty, 0 \leq y \leq s\}$. We aim to apply the Fourier transform directly to the differential equation and boundary conditions in order to arrive at a Wiener-Hopf formulation – this approach is called Jones's method by [19].

Let us define the jump in a quantity across the first cascade strip by $[\,\cdot\,]$, so that for instance the jump in unsteady pressure p is given by

$$[p]\,(x) = p(x, 0^+) - e^{-i\sigma} p(x + d, s^-), \tag{9}$$

and use the following convention for the x-wise Fourier transform:

$$\Phi(\alpha, y) := \int_{-\infty}^{\infty} e^{i\alpha x}\phi(x, y)dx.$$

Fourier transforming Eq. (2) and boundary condition (v) we find

$$\frac{\partial^2\Phi}{\partial^2 y}(\alpha, y) - \gamma^2(\alpha)\Phi(\alpha, y) = 0 \tag{10}$$

$$\frac{\partial\Phi}{\partial y}(\alpha, 0^+) - e^{-i\sigma - id\alpha}\frac{\partial\Phi}{\partial y}(\alpha, s^-) = 0, \tag{11}$$

where $\gamma^2(\alpha) = \alpha^2\beta^2 + 2\alpha\tilde{\Omega}M_xM - \left(\tilde{\Omega}^2M^2 - K_3^2\right)$ and the branch cuts of γ are chosen such that the function always has positive real part. We also note that the Fourier transform of the pressure fluctuations is related to the Fourier-transformed velocity potential by

$$P(\alpha, y) = -\left(i\tilde{\Omega}\frac{M}{M_x} - i\alpha\right)\Phi(\alpha, y)$$

$$[P](\alpha) = -\left(i\tilde{\Omega}\frac{M}{M_x} - i\alpha\right)[\Phi](\alpha). \tag{12}$$

We can solve Eq. (10) to yield $\Phi(\alpha, y) = A(\alpha)\exp(\gamma(\alpha)y) + B(\alpha)\exp(-\gamma(\alpha)y)$ and imposing the periodicity Eq. (11) together with Eq. (12) implies after a few steps of algebra that

$$[P](\alpha) = \kappa(\alpha)\frac{\partial\Phi}{\partial y}(\alpha, 0), \tag{13}$$

where

$$\begin{aligned}\kappa(\alpha) &= \frac{2\left(\tilde{\Omega}\frac{M}{M_x} - \alpha\right)(\cos(\sigma + d\alpha) - \cosh(\gamma s))}{i\gamma\sinh(\gamma s)} \\ &= \frac{\left(\tilde{\Omega}\frac{M}{M_x} - \alpha\right)}{i\gamma\sinh(\gamma s)}\left(1 - e^{-i\sigma - \gamma s - id\alpha}\right)\left(1 - e^{-i\sigma + \gamma s - id\alpha}\right)e^{i\sigma + id\alpha}.\end{aligned}$$

We observe that $\kappa(\alpha)$ is single-valued in the complex plane, since its direct dependence on γ is even.

3.1. The multiplicative kernel κ

One can easily check (see for instance Peake [8]) that κ is meromorphic, with simple poles located at $\alpha = k_n^{\pm}, n \in \mathbb{N}$ where

$$k_n^{\pm} = \begin{cases} \frac{-M_xM\tilde{\Omega} \mp \sqrt{M_x^2M^2\tilde{\Omega}^2 - \beta^2(n^2\pi^2s^{-2} + K_3^2 - M^2\tilde{\Omega}^2)}}{\beta^2} & \text{if } n \le p \\ \frac{-M_xM\tilde{\Omega} \pm i\sqrt{-M_x^2M^2\tilde{\Omega}^2 + \beta^2(n^2\pi^2s^{-2} + K_3^2 - M^2\tilde{\Omega}^2)}}{\beta^2} & \text{if } n > p, \end{cases}$$

and p is the largest integer such that $M_x^2 M^2 (\mathrm{Re}\,\tilde{\Omega})^2 - \beta^2 (n^2\pi^2 s^{-2} + K_3^2 - M^2(\mathrm{Re}\,\tilde{\Omega})^2) \geq 0$. Furthermore κ has simple zeros at the convected wavenumber $\alpha = \tilde{\Omega}\frac{M}{M_x}$ and at $\alpha = \sigma_m^{\pm}, m \in \mathbb{Z}$, where for $-r \leq m \leq q$:

$$\sigma_m^{\pm} = \frac{-(s^2 M_x M\tilde{\Omega} + d\sigma + 2d\pi m)}{s^2\beta^2 + d^2} \mp \frac{\sqrt{\left(s^2 M_x M\tilde{\Omega} + d\sigma + 2d\pi m\right)^2 - (s^2\beta^2 + d^2)\left((\sigma + 2\pi m)^2 - s^2\left(\tilde{\Omega}^2 M^2 - K_3^2\right)\right)}}{s^2\beta^2 + d^2},$$

and for $m > q, m < -r$:

$$\sigma_m^{\pm} = \frac{-(s^2 M_x M\tilde{\Omega} + d\sigma + 2d\pi m)}{s^2\beta^2 + d^2} \pm \frac{i\sqrt{-\left(s^2 M_x M\tilde{\Omega} + d\sigma + 2d\pi m\right)^2 + (s^2\beta^2 + d^2)\left((\sigma + 2\pi m)^2 - s^2\left(\tilde{\Omega}^2 M^2 - K_3^2\right)\right)}}{s^2\beta^2 + d^2},$$

with $-r, q$ being the smallest and largest integer respectively such that

$$\left(s^2 M_x M(\mathrm{Re}\,\tilde{\Omega}) + d\sigma + 2d\pi m\right)^2 - (s^2\beta^2 + d^2)\left((\sigma + 2\pi m)^2 - s^2\left((\mathrm{Re}\,\tilde{\Omega})^2 M^2 - K_3^2\right)\right) \geq 0.$$

We call $k_n^{\pm}$ the duct modes (which are cut-on if and only if $n \leq p$) and $\sigma_m^{\pm}$ the radiation modes (which are cut-on if and only if $-r \leq m \leq q$). These are the acoustic modes that appear in this geometry, and $\alpha = \tilde{\Omega}\frac{M}{M_x}$ is the hydrodynamic mode supporting the wake downstream of the blades.

Incident acoustic waves

For acoustic waves we can verify using the parametrisation Eq. (6)-(8) that

$$K_1 = \begin{cases} \sigma_0^- & \text{if } s(M_x + \sin\theta\cos\varphi) - d\sin\theta\sin\varphi \geq 0 \\ \sigma_0^+ & \text{if } s(M_x + \sin\theta\cos\varphi) - d\sin\theta\sin\varphi < 0 \end{cases}$$

i.e. $K_1 = \sigma_0^-$ if the incident wave is travelling downstream with respect to the cascade stagger (i.e. is incident from upstream), and $K_1 = \sigma_0^+$ if the wave travels upstream (i.e. is incident from downstream). For simplicity we restrict our analysis to the case of incident waves from upstream (i.e. for acoustic waves when $K_1 = \sigma_0^-$), but the scattering problem can be solved in an analogous (reflected) way in the case of upstream travelling waves incident from downstream as well.

3.2. Derivation of Wiener-Hopf equations

A convenient notation is

$$\tilde{\sigma}_m^- = \begin{cases} \tilde{\Omega}\frac{M}{M_x}, & \text{if } m = 0, \\ \sigma_{m-1}^-, & \text{if } m \geq 1 \\ \sigma_m^-, & \text{if } m \leq -1 \end{cases} \quad \text{and} \quad \tilde{\sigma}_m^+ = \sigma_m^+, \text{for all } m \in \mathbb{Z},$$

which allows us to write the Neumann boundary condition for incident acoustic and vorticity waves as

$$\frac{\partial \phi}{\partial y} = -V_g e^{in\sigma - i\tilde{\sigma}_\eta^- x} \text{ on } \{0 \leq x - nd \leq 1, y = ns\},$$

where our analysis facilitates a solution for any $-r \leq \eta \leq q$ and in particular for the physically relevant values $\eta = 0, 1$, which correspond to incident gusts and incident (downstream travelling) acoustic waves respectively.

We follow the standard practise of assuming that $\tilde{\Omega}$ has a small negative imaginary part $\operatorname{Im}\tilde{\Omega} < 0$, which will at the end of the analysis be taken to zero. By construction this introduces a small negative imaginary part for both types of incident fields, and physically amounts to a small amount of damping downstream (for both a harmonic gust, and a downstream travelling acoustic wave) and ensures that certain integral transforms in the later analysis are well-defined.

We begin by deriving the system of Wiener-Hopf equations which we shall use to solve the problem. We use an approach similar to [11] (although we are able to reduce the number of equations from four to three) and split the boundary value problem into three problems on $\{-\infty < x < \infty, 0 \leq y \leq s\}$, each of which has to satisfy only a combination of two semi-infinite boundary conditions – hence making an application of the Wiener-Hopf technique possible. We define ϕ_1, ϕ_2, ϕ_3, each to satisfy Eq. (2) on the first cascade strip (i.e. on the space between the first and second blade of the cascade, $\{-\infty < x < \infty, 0 \leq y \leq s\}$), the radiation condition (iii) and the continuity of the blade-normal velocity everywhere (v) (which translates to the jump in normal velocity across the first cascade strip, as defined in Eq. (9), being zero). Finally we impose the following pairs of semi-infinite boundary conditions (together with an appropriate distribution of the edge conditions (vi)) on ϕ_i and the corresponding pressures $p_i, i = 1, 2, 3$:

- Leading-edge interaction with incident field:

$$\frac{\partial \phi_1}{\partial y}(x, 0) = -V_g e^{-i\tilde{\sigma}_\eta^- x} \text{ on } x > 0,$$
$$[p_1](x) = 0 \text{ on } x < 0,$$

  and ϕ_1 has the conventional inverse square-root singularity at the leading edge $x = 0$.

- Trailing-edge correction:

$$\frac{\partial \phi_2}{\partial y}(x, 0) = 0 \text{ on } x < 1,$$
$$[p_1 + p_2 + p_3](x) = 0 \text{ on } x > 1,$$

  and ϕ_2 satisfies the Kutta condition at the trailing edge $x = 1$.

- Leading-edge correction:

$$\frac{\partial \phi_3}{\partial y}(x,0) = 0 \text{ on } x > 0,$$
$$[p_2 + p_3](x) = 0 \text{ on } x < 0,$$

  and ϕ_3 has at worst an inverse square-root singularity at the leading edge $x = 0$.

Thus ϕ_1 corresponds to the scattered potential of a wave incident on a cascade of *semi-infinite* blades, while ϕ_2, ϕ_3 act jointly to correct the pressure jumps downstream of the trailing edge and to ensure that $\phi = \phi_1 + \phi_2 + \phi_3$ is a solution to the original problem. Since the derivation of Eq. (13) relied only on the time-reduced convected wave-equation, together with the radiation condition and the continuity of normal velocity, we find that each of $\phi_j, j = 1, 2, 3$ satisfies Eq. (13) as well. If we then transform the additional boundary conditions we arrive at the following system of scalar Wiener-Hopf equations:

$$\frac{\left[P_1^+\right](\alpha)}{\kappa(\alpha)} = \frac{\partial \Phi_1^-}{\partial y}(\alpha, 0) - \frac{iV_g}{\alpha - \tilde{\sigma}_\eta^-} \tag{14}$$

$$\frac{\partial \tilde{\Phi}_2^+}{\partial y}(\alpha, 0) = \frac{1}{\kappa(\alpha)} \left(\left[\tilde{P}_2^-\right](\alpha) - \left[\tilde{P}_1^+\right](\alpha) - \left[\tilde{P}_3^+\right](\alpha) \right) \tag{15}$$

$$\frac{\partial \Phi_3^-}{\partial y}(\alpha, 0) = \frac{1}{\kappa(\alpha)} \left(\left[P_3^+\right](\alpha) - \left[P_2^-\right](\alpha) \right), \tag{16}$$

where we used the following notation of half-line Fourier transforms for a given function ψ:

$$\Psi^+(\alpha, y) := \int_0^\infty e^{i\alpha x} \psi(x, y) dx, \qquad \Psi^-(\alpha, y) := \int_{-\infty}^0 e^{i\alpha x} \psi(x, y) dx,$$
$$\tilde{\Psi}^+(\alpha, y) := e^{-i\alpha} \int_1^\infty e^{i\alpha x} \psi(x, y) dx, \qquad \tilde{\Psi}^-(\alpha, y) := e^{-i\alpha} \int_{-\infty}^1 e^{i\alpha x} \psi(x, y) dx.$$

4. Solution using the Wiener-Hopf technique

Factorisation of κ

Given $\operatorname{Im} \tilde{\Omega} < 0$ there is ϵ such that $\pm \operatorname{Im} \tilde{\sigma}_m^\pm > \epsilon$ and $\pm \operatorname{Im} k_n^\pm > \epsilon$. Defining the overlapping half-planes $R^\pm := \left\{ \alpha \in \mathbb{C} \middle| \pm \operatorname{Im} \alpha > -\epsilon \right\}$ we observe that each of Eq. (14)-(16) is valid in the strip $R^+ \cap R^-$ and we note that the half-line Fourier transforms are analytic in $R^\pm$ according to their superscripts (under the a-priori assumption that the solutions ϕ_1, ϕ_2, ϕ_3 decay sufficiently fast along the x-direction).

Using the Weierstrass factorisation theorem (see theorem 5.14 in [20, p. 170] or the special case given in [19, p. 40]), and applying the procedure for analysing the asymptotic behaviour of infinite products as outlined by [19], it is possible

to construct functions κ^+, κ^- which are analytic in R^+, R^- respectively, satisfy $\kappa = \kappa^+\kappa^-$, and have the following algebraic growth behaviour:

$$\left|\kappa^+(\alpha)\right| \sim C^+|\alpha|^{\frac{1}{2}} \text{ as } \alpha \to \infty \text{ in } R^+ \tag{17}$$

$$\left|\kappa^-(\alpha)\right| \sim C^-|\alpha|^{-\frac{1}{2}} \text{ as } \alpha \to \infty \text{ in } R^- \tag{18}$$

for some non-zero constants $C^{\pm}$. The details of this splitting are described in Appendix A.

4.1. The uncoupled leading edge problem

We notice that Eq. (14) is uncoupled from the remaining two Wiener-Hopf equations. The equation corresponds essentially to the scattering problem on a cascade of semi-infinite blades, and explicit solutions have been provided by a number of authors. Amongst the earliest work on this problem is Carlson and Heins [2], and solutions are also given by Mani and Horvay [21], Glegg [11], and Peake [8]. Here we briefly summarise the main steps taken by Peake in the solution of this uncoupled problem (see [8, pp. 267-273]). Using the aforementioned kernel factorisation we can rewrite Eq. (14) in the form

$$\begin{aligned}\frac{\left[P_1^+\right](\alpha)}{\kappa^+(\alpha)} + \frac{iV_g\kappa^-(\tilde{\sigma}_\eta^-)}{\alpha - \tilde{\sigma}_\eta^-} &= \kappa^-(\alpha)\frac{\partial\Phi_1^-}{\partial y}(\alpha, 0) - \kappa^-(\alpha)\frac{iV_g}{\alpha - \tilde{\sigma}_\eta^-}\left(1 - \frac{\kappa^-(\tilde{\sigma}_\eta^-)}{\kappa^-(\alpha)}\right) \\ &= E_1(\alpha)\end{aligned} \tag{19}$$

which is valid in $R^+ \cap R^-$. Thus analytic continuation allows us to define an entire function $E_1(\alpha)$. As mentioned above we assume that the unsteady field ϕ_1 possesses the conventional inverse square-root singularity (condition (vi) from §2.1) at the leading edge $x = 0$, which results in the following asymptotic behaviour [8, p. 269]:

$$\begin{aligned}\frac{\partial\Phi_1^-}{\partial y}(\alpha, 0) &= \mathcal{O}\left(\alpha^{-\frac{1}{2}}\right) \text{ as } \alpha \to \infty \text{ in } R^-, \\ \left[P_1^+\right](\alpha) &= \mathcal{O}\left(\alpha^{-\frac{1}{2}}\right) \text{ as } \alpha \to \infty \text{ in } R^+.\end{aligned}$$

This inverse square-root singularity is a direct consequence of the flow being effectively incompressible and therefore satisfying Laplace's equation nearby the leading edge. This behaviour, together with Liouville's theorem, implies $E_1(\alpha) \equiv 0$ and therefore yields the solution to Eq. (14)

$$\begin{aligned}\left[P_1^+\right](\alpha) &= -iV_g\kappa^-(\tilde{\sigma}_\eta^-)\frac{\kappa^+(\alpha)}{\alpha - \tilde{\sigma}_\eta^-}, \\ \frac{\partial\Phi_1^-}{\partial y}(\alpha, 0) &= \frac{iV_g}{\alpha - \tilde{\sigma}_\eta^-}\left(1 - \frac{\kappa^-(\tilde{\sigma}_\eta^-)}{\kappa^-(\alpha)}\right).\end{aligned} \tag{20}$$

4.2. Asymptotic behaviour of the kernel factors and their residues

Before we can solve Eq. (15) and Eq. (16) we first need to look more closely at the asymptotic behaviour of the kernel factors $\kappa^{\pm}$ and their residues. We find that $|\kappa|$ has two asymptotic regimes - one regime with constant asymptotic behaviour, and one with exponential growth:

- As $\alpha \to \infty$ with $\pm \arg \alpha \in \left(\arctan\left(\frac{s\beta}{d}\right), \frac{\pi}{2}\right) \cup \left(\frac{\pi}{2}, \pi - \arctan\left(\frac{s\beta}{d}\right)\right)$

$$|\kappa(\alpha)| \sim \frac{2e^{d|\operatorname{Im}\alpha| - \beta s|\operatorname{Re}\alpha|}}{\beta}.$$

- And as $\alpha \to \infty$ with $\arg \alpha \in \left(-\arctan\left(\frac{s\beta}{d}\right), \arctan\left(\frac{s\beta}{d}\right)\right)$ or $\arg \alpha \in \left(\pi - \arctan\left(\frac{s\beta}{d}\right), \pi + \arctan\left(\frac{s\beta}{d}\right)\right)$,

$$|\kappa(\alpha)| \sim \frac{2}{\beta}.$$

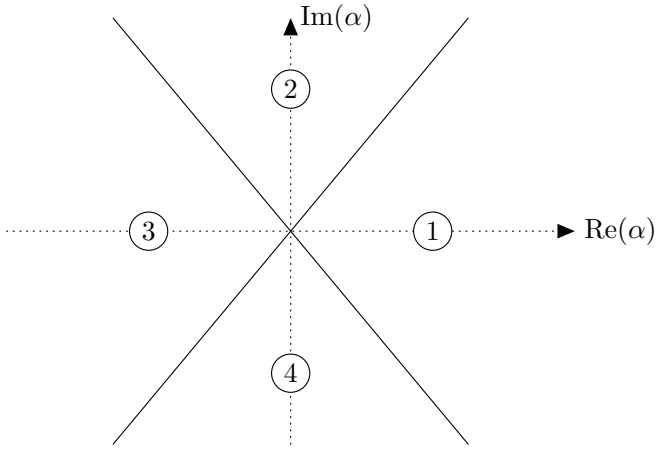

Figure 2: The regions of different asymptotic behaviour of $|\kappa|$ in the complex α-plane.

These regimes are sketched in figure 2: $|\kappa|$ has exponential growth at infinity in regions (2) and (4) and is asymptotically constant in regions (1) and (3). Now since κ^+ can be expressed in R^- by $\kappa^+ = \frac{\kappa}{\kappa^-}$, this means that κ^+ is not only of algebraic growth in R^+ but in fact in the following larger part of the complex plane

$$R^+ \cup \left\{\alpha \middle| \arg \alpha \in \left(-\arctan\left(\frac{s\beta}{d}\right), \arctan\left(\frac{s\beta}{d}\right)\right) \cup \left(\pi - \arctan\left(\frac{s\beta}{d}\right), \pi + \arctan\left(\frac{s\beta}{d}\right)\right)\right\},$$

which corresponds to a strip around the real axis together with regions (1), (2) and (3). An analogous statement is true for κ^-. Furthermore one finds that $\frac{1}{\kappa^+}$ is a meromorphic function, with simple poles and growth of order $\mathcal{O}\left(\alpha^{-\frac{1}{2}}\right)$ away from its poles (because either it decays algebraically or it decays exponentially).

In order to understand the poles of $\kappa^\pm$, $\frac{1}{\kappa^\pm}$ it suffices – by way of expressing the functions as above – to understand the residues of κ, $\frac{1}{\kappa}$. We can quickly check that for each $m \in \mathbb{Z}$, $n \in \mathbb{N}$:

$$\operatorname{Res}\left(\frac{1}{\kappa}, \sigma_m^+\right) = \frac{i\gamma(\sigma_m^+)^2}{(-2)(\tilde{\Omega}\frac{M}{M_x} - \sigma_m^+)\left(id\gamma(\sigma_m^+) + s\sigma_m^+\right)}, \tag{21}$$

$$\operatorname{Res}\left(\frac{1}{\kappa}, \sigma_m^-\right) = \frac{i\gamma(\sigma_m^-)^2}{2(\tilde{\Omega}\frac{M}{M_x} - \sigma_m^-)\left(id\gamma(\sigma_m^-) - s\sigma_m^-\right)}, \tag{22}$$

$$\operatorname{Res}\left(\kappa, k_n^+\right) = \frac{2(\tilde{\Omega}\frac{M}{M_x} - k_n^+)(cos(\sigma + dk_n^+) - (-1)^n)}{(-1)^n ik_n^+ s}, \tag{23}$$

$$\operatorname{Res}\left(\kappa, k_n^-\right) = \frac{2(\tilde{\Omega}\frac{M}{M_x} - k_n^-)(cos(\sigma + dk_n^-) - (-1)^n)}{(-1)^n ik_n^- s}. \tag{24}$$

4.3. The trailing edge correction

We can rewrite Eq. (15) as

$$\kappa^+(\alpha)\frac{\partial\tilde{\Phi}_2^+}{\partial y}(\alpha, 0) = \frac{1}{\kappa^-(\alpha)}\left(\left[\tilde{P}_2^-\right](\alpha) - \left[\tilde{P}_1^+\right](\alpha) - \left[\tilde{P}_3^+\right](\alpha)\right).$$

Thus to proceed with the Wiener-Hopf technique we must additively split the term

$$g(\alpha) = \frac{1}{\kappa^-(\alpha)}\left(\left[\tilde{P}_1^+\right](\alpha) + \left[\tilde{P}_3^+\right](\alpha)\right).$$

We now recall from Eq. (18) that $\frac{1}{\kappa^-}$ is of order $\mathcal{O}\left(\alpha^{\frac{1}{2}}\right)$ uniformly in some strip containing the real axis, i.e. in a set of the form $(-\infty, \infty) \times (-\epsilon, \epsilon)$, such that $(-\infty, \infty) \times [-\epsilon, \epsilon] \subset R^+ \cap R^-$. It is also possible to show (as is proved in detail in Appendix B) that

$$\left[\tilde{P}_1^+\right](\alpha) = \mathcal{O}\left(\alpha^{-1}\right)$$

as $\alpha \to \infty, \alpha \in R^+$, and hence that $[p_1]$ is non-singular at $x = 1$. Imposing the unsteady Kutta condition (condition (vi) in §2.1) at the trailing edge to $[p_2]$ and noting that $[p_3](x) = -[p_1](x) - [p_2](x)$, for $x > 1$, we conclude that the pressure jump $[p_3](x)$ must be non-singular at $x = 1$, and it can thus be shown that $\left[\tilde{P}_3^+\right](\alpha) = \mathcal{O}\left(\alpha^{-1}\right)$ as $\alpha \to \infty, \alpha \in R^+$. Hence there is a strip $\mathcal{S}$ containing the real axis and a constant C such that

$$\left|\frac{1}{\kappa^-(\alpha)}\left(\left[\tilde{P}_1^+\right](\alpha) + \left[\tilde{P}_3^+\right](\alpha)\right)\right| \leq C\left(1 + |\operatorname{Re}\alpha|\right)^{-\frac{1}{2}}, \text{ for all } \alpha \in \mathcal{S}.$$

Thus the assumptions of theorem B in [19, p. 13] are satisfied and we can choose $c > 0$ and construct two functions such that $g = g_- + g_+$, where

$$g_+(\alpha) = \frac{1}{2\pi i}\int_{-\infty-ic}^{\infty-ic} \frac{g(\zeta)}{\zeta-\alpha}d\zeta \text{ and } g_-(\alpha) = \frac{1}{2\pi i}\int_{-\infty+ic}^{\infty+ic} \frac{g(\zeta)}{\zeta-\alpha}d\zeta.$$

Let us shrink $R^{\pm}$ such that

$$R^- = \left\{\alpha \in \mathbb{C}\middle|\, \operatorname{Im}\alpha < \delta\right\} \text{ and } R^+ = \left\{\alpha \in \mathbb{C}\middle|\, \operatorname{Im}\alpha > -\delta\right\}$$

for some $0 < \delta < c$, then the functions $g_\pm$ are analytic in $R^\pm$ respectively. Furthermore they are also bounded in their respective half-plane, as is proved in Appendix B. We now observe that $\frac{g(\zeta)}{\zeta-\alpha}$ is meromorphic in an open neighbourhood of $\{\zeta\big|\, \operatorname{Im}\zeta \geq -c\}$, with simple poles at $\sigma_m^+, m \in \mathbb{Z}$ and, by Eq. (17)-(18), decay of $\mathcal{O}\left(\alpha^{-\frac{3}{2}}\right)$. Thus we can use the residue theorem to express $g_-(\alpha)$ in terms of the following infinite series of pole contributions:

$$g_-(\alpha) = \sum_{m\in\mathbb{Z}} \frac{1}{\alpha-\sigma_m^+} \operatorname{Res}\left(\frac{1}{\kappa^-}, \sigma_m^+\right)\left(\left[\tilde{P}_1^+\right](\sigma_m^+) + \left[\tilde{P}_3^+\right](\sigma_m^+)\right). \tag{25}$$

At this point we wish to highlight that the splitting derived in Eq. (25) is new and different to previous methods. Indeed the corresponding splitting used in previous studies (for instance Peake [8] and Glegg [11]) relies essentially on the following observation: If $d < 1$ then $[p_1](x) + [p_3](x), x > 1$, can be written as an (infinite) linear combination of duct modes k_n^-. This is because in the region $x > 1$ the consecutive semi-infinite boundary conditions form a duct geometry (cf. §3.2). Thus, when $d < 1$, their half-line Fourier transform is of the form

$$\left[\tilde{P}_1^+\right](\alpha) + \left[\tilde{P}_3^+\right](\alpha) = \sum_{n\in\mathbb{N}} \frac{L_n}{\alpha - k_n^-} \tag{26}$$

for some complex constants L_n. With this knowledge one can close the contour of integration of $g_+(\alpha)$ in the lower half plane and derive a linear system from the discrete pole contributions at the duct modes $k_n^-, n \in \mathbb{N}$. However Eq. (26) is no longer valid when $d > 1$, because the modal structure of the pressure $[p_1](x) + [p_3](x)$ becomes more complicated in the region $1 < x < d$, since there is no overlap of consecutive boundary conditions in this part of the domain. As such the additive splitting and linear system from previous work are restricted to the case $d < 1$. We observe, however, that no such assumption was necessary to arrive at Eq. (25), indeed collecting the pole contributions at the radiation modes avoids making a distinction between overlapping and non-overlapping geometries altogether and forms a valid splitting for any value of $d > 0$. Now we note by Eq. (21), and Eq. (A.1)-(A.2), that the series in Eq. (25) converges locally uniformly in $\alpha \in R^-$ (since the terms in the series decay like $m^{-3/2}$).

This allows us to recast Eq. (15) into

$$\begin{aligned}\kappa^+(\alpha)\frac{\partial\tilde{\Phi}_2^+}{\partial y}(\alpha,0)+g_1^+(\alpha) &= \frac{1}{\kappa^-(\alpha)}\left[\tilde{P}_2^-\right](\alpha)\\ &\quad-\sum_{m\in\mathbb{Z}}\frac{1}{\alpha-\sigma_m^+}\operatorname{Res}\left(\frac{1}{\kappa^-},\sigma_m^+\right)\left(\left[\tilde{P}_1^+\right](\sigma_m^+)+\left[\tilde{P}_3^+\right](\sigma_m^+)\right)\\ &= E_2(\alpha),\end{aligned}$$

which by analytic extension defines an entire function $E_2(\alpha)$. By the unsteady Kutta condition at the trailing edge, both the normal velocity and the pressure field are non-singular at $x=1, y=0$. Thus there is a constant C such that

$$\begin{aligned}\left|\frac{\partial\tilde{\Phi}_2^+}{\partial y}(\alpha,0)\right| &\le \frac{C}{1+|\operatorname{Im}\alpha|} \quad \text{if } \alpha\in R^+\\ \left|\left[\tilde{P}_2^-\right](\alpha)\right| &\le \frac{C}{1+|\operatorname{Im}\alpha|} \quad \text{if } \alpha\in R^-,\end{aligned}$$

which implies together with our previous analysis that $|E_2(\alpha)|\le C|\alpha|^{\frac{1}{2}}$ uniformly in $\mathbb{C}$, and thus by the extended Liouville theorem $E_2(\alpha)$ must be constant. Moreover, $E_2(iy)\to 0$ as $y\to-\infty$ and thus E_2 must be identically zero, which then implies:

$$\frac{1}{\kappa^-(\alpha)}\left[\tilde{P}_2^-\right](\alpha)=\sum_{m\in\mathbb{Z}}\frac{1}{\alpha-\sigma_m^+}\operatorname{Res}\left(\frac{1}{\kappa^-},\sigma_m^+\right)\left(\left[\tilde{P}_1^+\right](\sigma_m^+)+\left[\tilde{P}_3^+\right](\sigma_m^+)\right). \tag{27}$$

4.4. The leading edge correction

We proceed similarly to the trailing edge correction: Firstly note that Eq. (16) is equivalent to

$$\kappa^-(\alpha)\frac{\partial\Phi_3^-}{\partial y}(\alpha,0)=\frac{1}{\kappa^+(\alpha)}\left(\left[P_3^+\right](\alpha)-\left[P_2^-\right](\alpha)\right).$$

Thus we must additively split the term

$$h(\alpha)=\frac{1}{\kappa^+(\alpha)}\left[P_2^-\right](\alpha).$$

We now observe that by construction $[p_2](x)=-[p_3](x)$, for $x<0$. Additionally we assumed that $[p_3](x)$ exhibits at worst the conventional inverse square-root singularity at the leading edge (cf. §3.2). Therefore $[p_2](x)$ must also have at worst an inverse square-root singularity at $x=0$ and thus $\left[P_2^-\right](\alpha)=\mathcal{O}\left(\alpha^{-1/2}\right)$ as $\alpha\to\infty, \alpha\in R^-$. This means that there is a strip $\mathcal{S}$ around the real axis and a constant C such that

$$|h(\alpha)|\le C\left(1+|\operatorname{Re}\alpha|\right)^{-\frac{1}{2}}.$$

Thus we may proceed as before to apply theorem B from [19, p. 13] and construct two functions h_+, h_- which are bounded and analytic in R^+, R^- respectively, and are given by

$$h_+(\alpha) = \frac{1}{2\pi i}\int_{-\infty-ic}^{\infty-ic} \frac{h(\zeta)}{\zeta-\alpha}d\zeta \text{ and } h_-(\alpha) = \frac{1}{2\pi i}\int_{-\infty+ic}^{\infty+ic} \frac{h(\zeta)}{\zeta-\alpha}d\zeta.$$

Since $\frac{h(\zeta)}{\zeta-\alpha}$ is a meromorphic function with simple poles in an open neighbourhood containing $\{\zeta \big| \operatorname{Im}\zeta \leq c\}$, we can use the residue theorem to collect the contributions of poles and express h_+ as the following convergent series:

$$h_+(\alpha) = \sum_{m\in\mathbb{Z}} \frac{1}{\alpha-\tilde{\sigma}_m^-} \operatorname{Res}\left(\frac{1}{\kappa^+}, \tilde{\sigma}_m^-\right) \left[P_2^-\right](\tilde{\sigma}_m^-),$$

which converges locally uniformly due to the decay in the residues. We highlight again that as in §4.3 this additive Wiener-Hopf splitting relying on radiation modes is the main difference to previous work by [8, 11], and is valid for all $d > 0$, hence overcomes the restriction to overlapping blades. Thus Eq. (16) is equivalent to

$$\begin{aligned}\kappa^-(\alpha)\frac{\partial\Phi_3^-}{\partial y}(\alpha,0) - h_-(\alpha) &= \frac{1}{\kappa^+(\alpha)}\left[P_3^+\right](\alpha) - \sum_{m\in\mathbb{Z}} \frac{1}{\alpha-\tilde{\sigma}_m^-} \operatorname{Res}\left(\frac{1}{\kappa^+}, \tilde{\sigma}_m^-\right) \left[P_2^-\right](\tilde{\sigma}_m^-)\\ &= E_3(\alpha).\end{aligned}$$

As for the previous two Wiener-Hopf equations this defines, by analytic continuation, an entire function $E_3(\alpha)$. We further assumed that ϕ_3 has at worst an inverse square root type singularity at the leading edge, which implies that the growth of $\frac{\partial\Phi_3^-}{\partial y}(\alpha,0)$, $\left[P_3^+\right](\alpha)$ in R^-, R^+ is similar to the corresponding growth of $\frac{\partial\Phi_1^-}{\partial y}(\alpha,0)$, $\left[P_1^+\right](\alpha)$ respectively, which amounts to (cf. §4.1)

$$\begin{aligned}\frac{\partial\Phi_3^-}{\partial y}(\alpha,0) &= \mathcal{O}\left(\alpha^{-\frac{1}{2}}\right) \text{ as } \alpha\to\infty \text{ in } R^-,\\ \left[P_3^+\right](\alpha) &= \mathcal{O}\left(\alpha^{-\frac{1}{2}}\right) \text{ as } \alpha\to\infty \text{ in } R^+.\end{aligned}$$

Thus the entire function $E_3(\alpha)$ is bounded. Furthermore if we take $\alpha\to\infty$ with $\arg\alpha = \pi/2$, then the RHS of the equation decays to zero, thus Liouville's theorem combined with this observation implies $E_3(\alpha)\equiv 0$. Therefore in particular

$$\frac{1}{\kappa^+(\alpha)}\left[P_3^+\right](\alpha) = \sum_{m\in\mathbb{Z}} \frac{1}{\alpha-\tilde{\sigma}_m^-} \operatorname{Res}\left(\frac{1}{\kappa^+}, \tilde{\sigma}_m^-\right) \left[P_2^-\right](\tilde{\sigma}_m^-). \tag{28}$$

5. Reduction to an infinite algebraic system

In order to reduce Eq. (20), (27) and (28) to a discrete matrix equation we define the following coefficients (for $m \in \mathbb{Z}$)

$$A_m := \left[\tilde{P}_1^+\right](\tilde{\sigma}_m^+),\ \ B_m := \left[P_2^-\right](\tilde{\sigma}_m^-),\ \ C_m := \left[\tilde{P}_3^+\right](\tilde{\sigma}_m^+).$$

Then using Eq. (27) we find by Fourier inversion and several changes of order of summation and integration, which are rigorously justified in Appendix C:

$$B_j = \left[P_2^-\right](\tilde{\sigma}_m^-) = \sum_{m\in\mathbb{Z}} \mathbf{G}_{jm}\left(A_m + C_m\right),$$

where

$$\mathbf{G}_{jm} = \frac{-1}{2\pi i}\int_{-\infty+i\epsilon}^{\infty+i\epsilon} \frac{1}{\alpha-\tilde{\sigma}_j^-} e^{i\alpha}\kappa^-(\alpha)\frac{1}{\alpha-\tilde{\sigma}_m^+}d\alpha\,\mathrm{Res}\left(\frac{1}{\kappa^-},\tilde{\sigma}_m^+\right). \tag{29}$$

and the contour of integration Γ^- behaves like $\arg\alpha \sim -\tilde{\epsilon}\,\mathrm{sign}(\mathrm{Re}\,\alpha), 0<\tilde{\epsilon}\ll 1$, at its tails. A sketch of Γ^- is shown in figure B.8. We can also use Fourier inversion on Eq. (28) (which is given in full detail in Appendix C) to arrive at a second collection of linear equations. This allows us to reduce the scattering problem to the following linear system:

$$B_j = \sum_{m\in\mathbb{Z}} \mathbf{G}_{jm}\left(A_m + C_m\right), \tag{30}$$

$$C_j = \sum_{m\in\mathbb{Z}} \mathbf{F}_{jm} B_m, \tag{31}$$

where $\mathbf{G}_{jm}$ are as in Eq. (32) and

$$\mathbf{F}_{jm} = \frac{1}{2\pi i}\int_{\Gamma^-} \frac{1}{\alpha-\tilde{\sigma}_j^+} e^{-i\alpha}\kappa^+(\alpha)\frac{1}{\alpha-\tilde{\sigma}_m^-}d\alpha\,\mathrm{Res}\left(\frac{1}{\kappa^+},\tilde{\sigma}_m^-\right), \tag{32}$$

In this system B_j, C_j are unknown coefficients which determine the solution to the scattering problem, while A_j are known and using the results from §4.1 we can express these as

$$A_j = \frac{-V_g}{2\pi}\int_{\Gamma^-} \frac{1}{\alpha-\tilde{\sigma}_j^+}\frac{1}{\alpha-\tilde{\sigma}_\eta^-} e^{-i\alpha}\kappa^+(\alpha)\kappa^-(\tilde{\sigma}_\eta^-)d\alpha,$$

where, as we outlined in §3.2, the incidence parameter η, takes values $-r \le \eta \le q$, with $\eta = 0$ corresponding to the case of an incident gust, and $\eta = 1$ corresponding to the case of an incident sound wave.

5.1. Stable formulation under $\operatorname{Im}\tilde{\Omega} \to 0^-$

We now wish to reduce the fictitious damping $\operatorname{Im}\tilde{\Omega}$ to zero. Note in the above analysis we chose the contours of integration in the system Eq. (30)-(31), i.e. the oriented curves Γ^- and $\operatorname{Im}\alpha = \epsilon$, such that all poles and zeros in R^+ are above the curves and all poles and zeros in R^- are below the curves. Therefore if we were to *fix our current contours of integration* and then considered the limit $\operatorname{Im}\tilde{\Omega} \to 0^-$, then the poles of the cut-on modes would have to cross the contours of integration in order to move onto the real-axis. In addition, if we allowed the contours of integration to change according to the above restrictions when $\operatorname{Im}\tilde{\Omega} \to 0^-$, then the contours would coalesce on the real axis (at least in a neighbourhood of the origin) and the poles corresponding to cut-on modes would end up on the contours. This means that our current contours (although appropriate for the analytical treatment) are not suitable for numerical evaluation in the physical case of zero damping (i.e. when $\operatorname{Im}\tilde{\Omega} = 0$). In order to overcome this problem we change contours of integration to a set of contours that allows us to evaluate the linear system numerically even when all the cut-on modes are located on the real-axis. Thus we consider the following change of contours: Choose $|\operatorname{Im}\tilde{\Omega}| = \delta$ sufficiently small such that there is a constant $\epsilon_1 > 0$ such that for all $0 \le \operatorname{Im}\tilde{\Omega} \le \delta$, we have $\operatorname{Im}\tilde{\Omega}\frac{M}{M_x} > -\epsilon_1$,

$$|\operatorname{Im}\sigma_m^{\pm}| < \epsilon_1, \text{ if } -r \le m \le q+1, \quad \text{and} \quad |\operatorname{Im}\sigma_m^{\pm}| > \epsilon_1, \text{ if } m > q+1, m < -r,$$

i.e. such that all cut-on modes are inside a strip of width $2\epsilon_1$ around the real axis, and all cut-off modes are outside. Then we can change the contours as follows, in each case picking up a pole contribution if the corresponding mode is cut-on:

$$\begin{aligned}
\mathbf{F}_{jm} &= \frac{1}{2\pi i}\int_{-\infty+i\epsilon_1}^{\infty+i\epsilon_1} \frac{1}{\alpha-\tilde{\sigma}_j^+} e^{-i\alpha}\kappa^+(\alpha)\frac{1}{\alpha-\tilde{\sigma}_m^-}d\alpha \operatorname{Res}\left(\frac{1}{\kappa^+}, \tilde{\sigma}_m^-\right) \\
&\quad + \operatorname{Res}\left(\frac{1}{\kappa^+}, \tilde{\sigma}_m^-\right)\begin{cases} e^{-i\tilde{\sigma}_j^+}\kappa^+(\tilde{\sigma}_j^+)\frac{1}{\tilde{\sigma}_j^+-\tilde{\sigma}_m^-}, & \text{if } \tilde{\sigma}_j^+ \text{ is cut-on} \\ 0, & \text{otherwise,} \end{cases} \\
\mathbf{G}_{jm} &= \frac{-1}{2\pi i}\int_{-\infty-i\epsilon_1}^{\infty-i\epsilon_1} \frac{1}{\alpha-\tilde{\sigma}_j^-} e^{i\alpha}\kappa^-(\alpha)\frac{1}{\alpha-\tilde{\sigma}_m^+}d\alpha \operatorname{Res}\left(\frac{1}{\kappa^-}, \tilde{\sigma}_m^+\right) \\
&\quad + \operatorname{Res}\left(\frac{1}{\kappa^-}, \tilde{\sigma}_m^+\right)\begin{cases} e^{i\tilde{\sigma}_j^-}\kappa^-(\tilde{\sigma}_j^-)\frac{1}{\tilde{\sigma}_j^--\tilde{\sigma}_m^+}, & \text{if } \tilde{\sigma}_j^- \text{ is cut-on} \\ 0, & \text{otherwise,} \end{cases}
\end{aligned}$$

$$\begin{aligned}
A_j &= -\frac{V_g}{2\pi}\int_{-\infty+i\epsilon_1}^{\infty+i\epsilon_1} \frac{1}{\alpha-\tilde{\sigma}_j^+}\frac{1}{\alpha-\tilde{\sigma}_\eta^-} e^{-i\alpha}\kappa^+(\alpha)\kappa^-(\tilde{\sigma}_\eta^-)d\alpha \\
&\quad - iV_g\begin{cases} e^{-i\tilde{\sigma}_j^+}\kappa^+(\tilde{\sigma}_j^+)\kappa^-(\tilde{\sigma}_\eta^-)\frac{1}{\tilde{\sigma}_j^+-\tilde{\sigma}_\eta^-}, & \text{if } \tilde{\sigma}_j^+ \text{ is cut-on} \\ 0, & \text{otherwise.} \end{cases}
\end{aligned}$$

In these new expressions we are able to take the limit $\operatorname{Im}\tilde{\Omega} \to 0^-$ while keeping the contour of integration fixed, thus allowing us to solve the resulting system without the fictitious damping (by setting $\operatorname{Im}\tilde{\Omega} = 0$).

5.2. Approximate solution of the linear system

The system Eq. (30)-(31) is equivalent to:

$$(I - \mathbf{GF})B = \mathbf{G}A, \tag{33}$$

$$C = \mathbf{F}B, \tag{34}$$

where I is the identity operator. For our numerical results in §7 we solve Eq. (33) approximately using the finite section method (truncation), together with a numerical approximation to the integral coefficients $\mathbf{F}, \mathbf{G}$. The precise version of the finite section method employed in our numerical examples as well as a convergence analysis is described in Appendix D.

6. Total unsteady lift and far-field behaviour

We can now use our solution to find expressions for the total unsteady lift and the form of the velocity potential in the far-field given an incident gust, $\eta = 0$, and an incident sound wave, $\eta = 1$.

6.1. Total unsteady lift

The total unsteady lift on a single blade is (recalling the boundary condition (ii))

$$\mathcal{L} = \int_0^1 [p](x)dx = \int_{-\infty}^{\infty} [p](x)dx = [P](0).$$

Given our solution we can evaluate this as follows: Again by the boundary condition (ii)

$$[P](\alpha) = \left[P_1^+\right](\alpha) + \left[P_2^+\right](\alpha) + \left[P_3^+\right](\alpha), \tag{35}$$

and we showed earlier that

$$\left[P_1^+\right](\alpha) = -iV_g\kappa^-(\tilde{\sigma}_\eta^-)\frac{\kappa^+(\alpha)}{\alpha - \tilde{\sigma}_\eta^-} \tag{36}$$

$$\left[P_3^+\right](\alpha) = \kappa^+(\alpha)\sum_{m\in\mathbb{Z}} \frac{1}{\alpha - \tilde{\sigma}_m^-} \operatorname{Res}\left(\frac{1}{\kappa^+}, \tilde{\sigma}_m^-\right) B_m. \tag{37}$$

Furthermore

$$\left[P_2^+\right](\alpha) = e^{i\alpha}\left[\tilde{P}_2^+\right](\alpha) + e^{i\alpha}\left[\tilde{P}_2^-\right](\alpha) - \left[P_2^-\right](\alpha), \tag{38}$$

and we can express these in terms of our known quantities A_m, B_m, C_m as follows (for Eq. (39), (42) & (43) we used Fourier inversion and then the appropriate forward half-transform):

$$\left[P_2^-\right](\alpha) = \sum_{m\in\mathbb{Z}} (A_m + C_m) \operatorname{Res}\left(\frac{1}{\kappa^-}, \tilde{\sigma}_m^+\right) \left(\frac{-1}{2\pi i}\right) \int_{-\infty+i\epsilon}^{\infty+i\epsilon} \frac{\kappa^-(\alpha')}{\alpha'-\alpha} \frac{e^{i\alpha'}}{\alpha'-\tilde{\sigma}_m^+} d\alpha' \tag{39}$$

$$\left[\tilde{P}_2^-\right](\alpha) = \kappa^-(\alpha) \sum_{m\in\mathbb{Z}} (A_m + C_m) \frac{1}{\alpha - \tilde{\sigma}_m^+} \operatorname{Res}\left(\frac{1}{\kappa^-}, \tilde{\sigma}_m^+\right) \tag{40}$$

$$\left[\tilde{P}_2^+\right](\alpha) = -\left[\tilde{P}_1^+\right](\alpha) - \left[\tilde{P}_3^+\right](\alpha) \tag{41}$$

$$\left[\tilde{P}_1^+\right](\alpha) = \frac{-iV_g}{2i\pi} \int_{-\infty-i\epsilon}^{\infty-i\epsilon} \frac{e^{-i\alpha'}}{\alpha'-\alpha} \frac{\kappa^+(\alpha')}{\alpha'-\tilde{\sigma}_\eta^-} \kappa^-(\tilde{\sigma}_\eta^-) d\alpha' \tag{42}$$

$$\left[\tilde{P}_3^+\right](\alpha) = \frac{1}{2i\pi} \sum_{m\in\mathbb{Z}} \operatorname{Res}\left(\frac{1}{\kappa^+}, \tilde{\sigma}_m^-\right) B_m \int_{\Gamma^-} \frac{e^{-i\alpha'}}{\alpha'-\alpha} \frac{\kappa^+(\alpha')}{\alpha'-\tilde{\sigma}_m^-} d\alpha'. \tag{43}$$

Similarly to §5.1 we can express the contour integrals in a form that is stable under $\operatorname{Im}\tilde{\Omega} \to 0^-$ and in summary the total unsteady lift has the following form which can be evaluated numerically:

$$\begin{aligned}
\mathcal{L} = {} & iV_g \kappa^-(\tilde{\sigma}_\eta^-) \frac{1}{2\pi i} \int_{-\infty+i\epsilon_1}^{\infty+i\epsilon_1} \frac{1}{\alpha} \frac{1}{\alpha - \tilde{\sigma}_\eta^-} e^{-i\alpha} \kappa^+(\alpha) d\alpha \\
& - \sum_{m\in\mathbb{Z}} \operatorname{Res}\left(\frac{1}{\kappa^+}, \tilde{\sigma}_m^-\right) B_m \frac{1}{2i\pi} \int_{-\infty+i\epsilon_1}^{\infty+i\epsilon_1} \frac{e^{-i\alpha}}{\alpha} \frac{\kappa^+(\alpha)}{\alpha - \tilde{\sigma}_m^-} d\alpha \\
& + \sum_{m\in\mathbb{Z}} (A_m + C_m) \operatorname{Res}\left(\frac{1}{\kappa^-}, \tilde{\sigma}_m^+\right) \frac{1}{2\pi i} \int_{-\infty-i\epsilon_1}^{\infty-i\epsilon_1} \frac{e^{i\alpha}}{\alpha} \frac{\kappa^-(\alpha)}{\alpha - \tilde{\sigma}_m^+} d\alpha.
\end{aligned}$$

Here $\epsilon_1 > 0$ is such that when $\operatorname{Im}\tilde{\Omega} = 0$ all cut-off modes lie outside the strip $|\operatorname{Im}\alpha| \le \epsilon_1$.

6.2. Far-field behaviour

We aim to understand the behaviour of the scattered potential ϕ far downstream ($x > 0, |x| \gg 1$) and far upstream ($x < 0, |x| \gg 1$) of the blades. To do so we observe the following identity, which follows after a few steps of algebra from Eq. (10) together with the periodicity Eq. (11) and the expression for the pressure Eq. (12):

$$\Phi(\alpha, y) = [P](\alpha) \frac{\cosh(\gamma y) e^{i\sigma + id\alpha} - \cosh(\gamma(y-s))}{\kappa(\alpha)\sinh(\gamma s)\gamma}.$$

Thus we can find the velocity potential ϕ by computing the inverse Fourier transform

$$\phi(x, y) = \frac{1}{2\pi} \int_{-\infty}^{\infty} e^{-i\alpha x} [P](\alpha) \frac{\cosh(\gamma y) e^{i\sigma + id\alpha} - \cosh(\gamma(y-s))}{\kappa(\alpha)\sinh(\gamma s)\gamma} d\alpha.$$

We can then express $[P]$ using Eq. (35)-(43). The resulting integrand when multiplied by $e^{-i\alpha x}$ decays exponentially in the upper half complex plane if $x < 0$, and decays exponentially in the lower half complex plane if $x > 1 + d$. In both cases we can then close the contour of integration, and collect the appropriate pole contributions which yield after a few steps of algebra and care when exchanging order of summation and integration:

Far field downstream

For $x > 1 + d$ and $0 \leq y \leq s$:

$$\begin{aligned}\phi(x,y) = \sum_{m\in\mathbb{Z}} e^{-ix\tilde{\sigma}_m^-} f_m(y)\,\mathrm{Res}\left(\frac{1}{\kappa},\tilde{\sigma}_m^-\right)\frac{1}{\gamma(\tilde{\sigma}_m^-)} \\ \Bigg[iB_m - i\sum_{l\in\mathbb{Z}}(A_l+C_l)e^{i\tilde{\sigma}_m^-}\,\mathrm{Res}\left(\frac{1}{\kappa^-},\tilde{\sigma}_l^+\right)\kappa^-(\tilde{\sigma}_m^-)\frac{1}{\tilde{\sigma}_m^- - \tilde{\sigma}_l^+} \\ -iV_g\kappa^-(\tilde{\sigma}_\eta^-)\frac{1}{2\pi}\int_{-\infty+i\epsilon_1}^{\infty+i\epsilon_1}\frac{e^{-i\alpha}}{\alpha-\tilde{\sigma}_\eta^-}\frac{\kappa^+(\alpha)}{\alpha-\tilde{\sigma}_m^-}d\alpha e^{i\tilde{\sigma}_m^-} \\ +\sum_{l\in\mathbb{Z}}\mathrm{Res}\left(\frac{1}{\kappa^+},\tilde{\sigma}_l^-\right)B_l e^{i\tilde{\sigma}_m^-}\frac{1}{2\pi}\int_{-\infty+i\epsilon_1}^{\infty+i\epsilon_1}\frac{e^{-i\alpha}}{\alpha-\tilde{\sigma}_l^-}\frac{\kappa^+(\alpha)}{\alpha-\tilde{\sigma}_m^-}d\alpha\Bigg],\end{aligned} \tag{44}$$

where $f_m(y) = \frac{\cosh\left(\gamma(\tilde{\sigma}_m^-)y\right)e^{i\sigma+id\tilde{\sigma}_m^-} - \cosh\left(\gamma(\tilde{\sigma}_m^-)(y-s)\right)}{\sinh\left(\gamma(\tilde{\sigma}_m^-)s\right)}$ which can be further simplified for the acoustic modes (i.e. when $m \neq 0$):

$$f_m(y) = \begin{cases} e^{\gamma(\sigma_{m-1}^-)y}, & \text{if } m \geq 1 \\ e^{\gamma(\sigma_m^-)y}, & \text{if } m < 0. \end{cases}$$

We observe that the far field downstream of the blades consists only of radiating modes that travel downstream, and a hydrodynamic mode $\tilde{\Omega}\frac{M}{M_x}$ which supports the wake.

Far field upstream

For $x < 0$ and $0 \leq y \leq s$:

$$\begin{aligned}\phi(x,y) = \sum_{m\in\mathbb{Z}} e^{-i\tilde{\sigma}_m^+ x}\,\mathrm{Res}\left(\frac{1}{\kappa},\tilde{\sigma}_m^+\right)\frac{-e^{-\gamma(\tilde{\sigma}_m^+)y}}{\gamma(\tilde{\sigma}_m^+)}\Bigg[V_g\kappa^-(\tilde{\sigma}_\eta^-)\frac{\kappa^+(\tilde{\sigma}_m^+)}{\tilde{\sigma}_m^+ - \tilde{\sigma}_\eta^-} \\ +\kappa^+(\tilde{\sigma}_m^+)\sum_{l\in\mathbb{Z}}\frac{1}{\tilde{\sigma}_m^+ - \tilde{\sigma}_l^-}B_l\,\mathrm{Res}\left(\frac{1}{\kappa^+},\tilde{\sigma}_l^-\right) \\ +\sum_{l\in\mathbb{Z}}(A_l+C_l)\frac{1}{2\pi}\,\mathrm{Res}\left(\frac{1}{\kappa^-},\tilde{\sigma}_l^+\right)\int_{-\infty-i\epsilon_1}^{\infty-i\epsilon_1}\frac{e^{i\alpha}}{\alpha-\tilde{\sigma}_l^+}\frac{\kappa^-(\alpha)}{\alpha-\tilde{\sigma}_m^+}d\alpha \\ -ie^{i\tilde{\sigma}_m^+}(A_m+C_m)\Bigg].\end{aligned} \tag{45}$$

Similarly to the far field downstream, the scattered potential upstream consist only of radiating modes which travel upstream. Moreover there is no contribution from the hydrodynamic mode, since there is no wake upstream of the blades.

7. Numerical examples and results

The expressions for total unsteady lift and far-field amplitudes which we derived in §6 allow us to provide numerical results on the effects of cascade geometry and incident-wave properties on the scattered potential. The effects of incidence angle, spanwise wave numbers and mean flow are studied in detail in [5, 7, 11] and we therefore do not aim to provide a comprehensive parametric study of these effects, but rather we show typical results that can be achieved using our method, with particular focus on the effect of blade spacing and of non-overlapping cascade geometries. Furthermore, we note that the effect of cross-flow W was absorbed in our definition of $\tilde{\Omega}$, so that a larger cross-flow simply results in a smaller value of the effective reduced frequency, and therefore we need not study the effect of cross-flow separately. We also provide examples that allow comparison to previous results in order to validate the accuracy of our method. Finally, we note that m, the number of equations retained when solving Eq. (33) using the finite section method (see §5.2), was chosen to ensure convergence in our numerical examples. The typical number chosen was $m \approx 70$, but for large mean flow significantly fewer equations were required whilst for small mean flow a larger number was retained ($m \approx 250$ when $M = \sqrt{M_x^2 + M_z^2} \approx 0.2$).

7.1. Total unsteady lift

For the total unsteady lift we begin by comparing our solution to results provided by Peake [10] for overlapping blades in a two-dimensional setting. For this we consider the same parameter settings as in [10, p. 269]: $M_z = 0, K_3 = 0, \eta = 0$ (i.e. an incident gust of reduced frequency Ω), $\tilde{\Omega} = \Omega = 1.0, \sigma = 2\pi/3, s = d = 1/\sqrt{2}, M = M_x \in [0.2, 0.9]$. The results can be seen in figures 3a and 3c and our solution appears to be in very good agreement with the reference result. The rapid variation observed in figure 3c corresponds to the first downstream radiating mode σ_0^- becoming cut-on. In figures 3b and 3d we plot the total unsteady lift in a case of non-overlapping blades (inaccessible to [10] and other previous work), with $s = d = \sqrt{2}$, and the remaining parameters as before. We observe overall a similar shape of the total lift. The increased blade spacing however has the effect of the radiating modes cutting on at lower Mach numbers which results in a rapid variation at $M \approx 0.55$ (corresponding to σ_0^- cutting on) and at $M \approx 0.85$ (corresponding to σ_1^- cutting on). Moreover, comparing figure 3c and figure 3d we can see that the amplitude of the unsteady lift is (almost always) reduced in the non-overlapping case, as would be expected for a more widely spaced cascade.

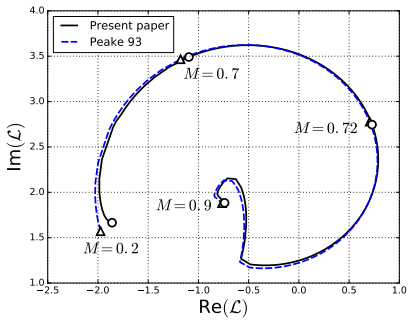

(a) $s = d = \frac{1}{\sqrt{2}}$.

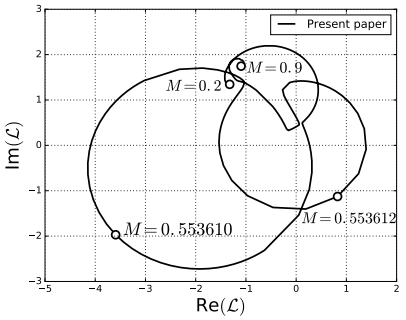

(b) $s = d = \sqrt{2}$.

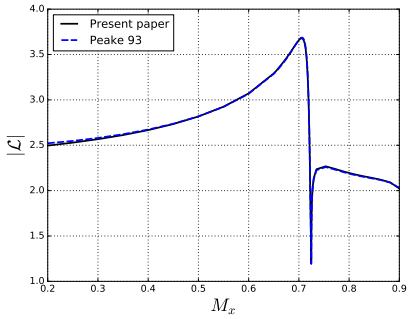

(c) $s = d = \frac{1}{\sqrt{2}}$.

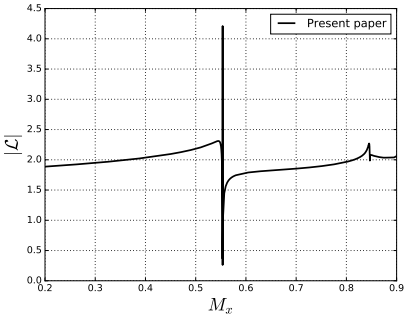

(d) $s = d = \sqrt{2}$.

Figure 3: Total lift $\mathcal{L}$ for $M \in [0.2, 0.9]$.

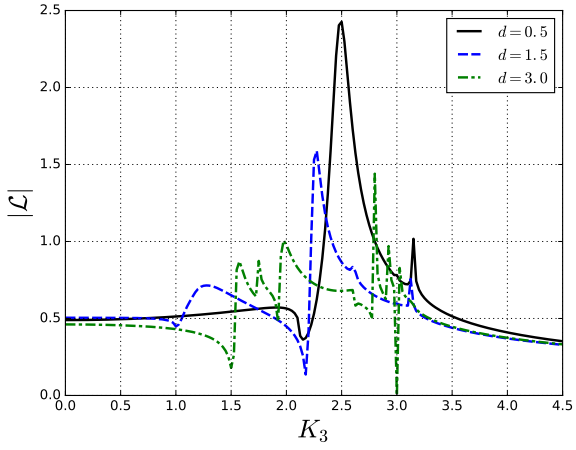

Figure 4: Total lift $|\mathcal{L}|$ as a function of K_3.

Next we study the effect of spanwise wavenumber on the total lift. We consider $M = M_x = 0.3, \tilde{\Omega} = \Omega = 10.0, \eta = 0$ (i.e. an incident gust), $\sigma = 3\pi/4, s \in \{0.6, 1.8, 3.6\}, \alpha = 5\pi/18$ and vary $K_3 \in [0, 4.5]$. The total unsteady lift is shown in figure 4 where in the black curve we can see the result for a case of overlapping blades and the remaining ones correspond to non-overlapping blades. In the case $d = 0.5$ the effect of K_3 is most apparent: From the formulae in §3.1 increasing K_3 sufficiently far has the effect of cutting off the acoustic modes. Indeed we observe a rapid variation in the lift around $K_3 \approx 2.4$ which is just after the radiating mode σ_0^- has cut off. For increased blade spacing we observe the interplay of this cut-off effect with increasing K_3 to the effect of more modes becoming cut-on as spacing increases. For $d = 3.0, K_3 = 0$ all of $\sigma_m^{\pm}, -2 \leq m \leq 2$, and $k_n^{\pm}, -3 \leq n \leq 3$, are cut-on, however as we increase K_3 they all cut off successively resulting in the rapid variations observed in the corresponding green curve. As we reach $K_3 = \frac{\Omega M_x}{\beta} \approx 3.14$ all of the acoustic modes have to become cut-off since by the dispersion relation Eq. (5) there are no propagating acoustic modes for $K_3 > \frac{\Omega M_x}{\beta}$. This is indeed observed in figure 4.

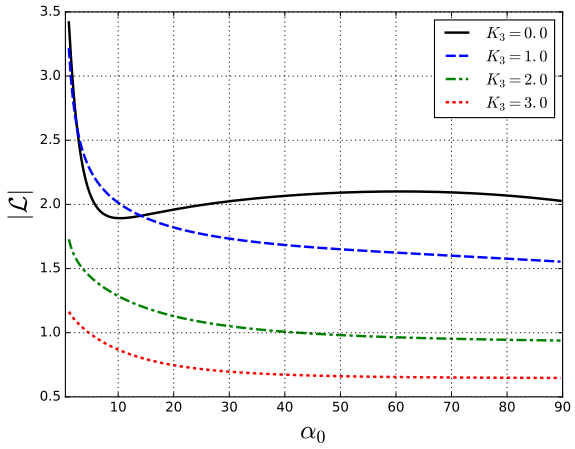

Figure 5: Total lift $|\mathcal{L}|$ as a function of α_0.

Finally, we consider the effect of the cascade stagger angle α_0 on the total lift. In figure 5 we see the dependence of the total unsteady lift on α_0, with $\sqrt{s^2 + d^2} = 1.5$ fixed. The remaining parameters were chosen as $M = M_x = 0.3, M_z = 0, \eta = 0, \sigma = 3\pi/4, \tilde{\Omega} = \Omega = 1.0, K_3 \in \{0, 1.0, 2.0, 3.0\}$. We note that here we have $d > 1$ for $\alpha_0 < 48.18°$. Most importantly we observe the smooth transition of $\mathcal{L}$ from the non-overlapping to the overlapping regime as α_0 increases from 0. We also observe an apparently singular behaviour as $\alpha_0 \to 0$, which corresponds to the limit of no vertical separation between the blades where our model is clearly invalid.

7.2. Far field behaviour

We now consider the far field sound for an incident acoustic wave as derived in §6.2. We begin by reproducing results given by Koch [7, p. 125], who considered the transmission and reflection amplitudes relative to the incident amplitude as a function of angle of incidence. In order to match Koch's settings we restrict ourselves to the case $M_z = 0, \theta = \pi/2$, which means we consider an incident acoustic wave ($\eta = 1$) with $K_1 = \frac{\tilde{\Omega} M \cos\varphi}{1+M_x \cos\varphi}, K_2 = \frac{\tilde{\Omega} M \sin\varphi}{1+M_x \cos\varphi}, K_3 = 0$. We further choose $(s,d) \in \{(\sin\alpha_0, \cos\alpha_0), (2\sin\alpha_0, 2\cos\alpha_0), (3\sin\alpha_0, 3\cos\alpha_0)\}$, $M = M_x \in \{0.3, 0.5, 0.7\}$, $k_0 = 0.25\pi, \alpha_0 = \pi/6$ and $\tilde{\Omega} = \Omega = k_0/M$. In figure 6 we show the transmission and reflection amplitudes relative to the incident amplitude V_0. These amplitudes $T_m, R_m, m \in \mathbb{Z}$, are such that

$$\phi(x,y) = \begin{cases} T_{\tilde{\Omega}\frac{M}{M_x}} e^{-ix\tilde{\Omega}\frac{M}{M_x}} f_0(y) + \sum_{m\in\mathbb{Z}} T_m e^{-ix\sigma_m^- + \gamma(\sigma_m^-)y} & x > d+1 \\ \sum_{m\in\mathbb{Z}} R_m e^{-i\sigma_m^+ x - \gamma(\sigma_m^+)y} & x < 0, \end{cases}$$

and they are explicitly given in Eq. (44) and (45). In order to match Koch's setting we plot the modal pressure corresponding to the first transmitted and reflected acoustic mode of the total field $\phi + \phi_{inc}$. In our case these are given by $P_0^t = i(\sigma_0^- - \tilde{\Omega}M/M_x)(T_0 + V_g), P_0^i = i(\sigma_0^- - \tilde{\Omega}M/M_x)V_g, P_0^r = i(\sigma_0^+ - \tilde{\Omega}M/M_x)R_0$.

The results are shown in comparison to a number of point values taken from [7] in figures 6a and 6b. Our solution is found to be in good agreement with the cited results, with the largest discrepancy between the present paper's and Koch's results occurring in the reflection amplitude at incident angles around $\varphi - \alpha_0 \approx 300°$. We are also able to show the corresponding results when the blade spacing is increased. The overall trend to be observed is an increase in $|P_0^t/P_0^i|$ and a decrease in $|P_0^r|/|P_0^i|$ as the blade spacing increases. The increased blade spacing also allows for more interesting effects to occur: We observe rapid variations in figures 6e and 6f when $M = 0.7$ around $\varphi - \alpha_0 \approx 190°, 247°$ which correspond to radiating and duct modes becoming cut-on. We also observe rapid variations in figures 6d and 6f in $\varphi - \alpha_0 < 180°$ and $\varphi - \alpha_0 > 360°$ which correspond to the first radiating modes σ_0^+, σ_0^- coalescing, which only takes place for sufficiently large blade spacing.

The effect of increased transmission and reduced reflection is further observed in our final result, which shows the relative transmission and reflection amplitudes for the modes $\sigma_0^-, \sigma_1^-, \sigma_0^+$ as a function of blade spacing. This result is shown in figure 7, where we consider a similar setting as in figure 6 with $M = M_x = 0.7, \varphi = 7\pi/6, \alpha_0 = \pi/6$ and vary $d \in [0.5, 6]$ with s/d fixed. The figure demonstrates two central effects of the increasing blade spacing on the far field: Firstly, the increase in spacing results in an increasing trend of $|T_0 + V_g|/|V_g|$ to 1 and a decreasing trend of all other amplitudes to 0. Secondly, as d increases, the radiating modes and duct modes become cut-on successively, resulting in the rapid variations observed in the graph. Both effects can be interpreted to mean that, as an acoustic obstacle, the cascade becomes more permeable as the spacing increases.

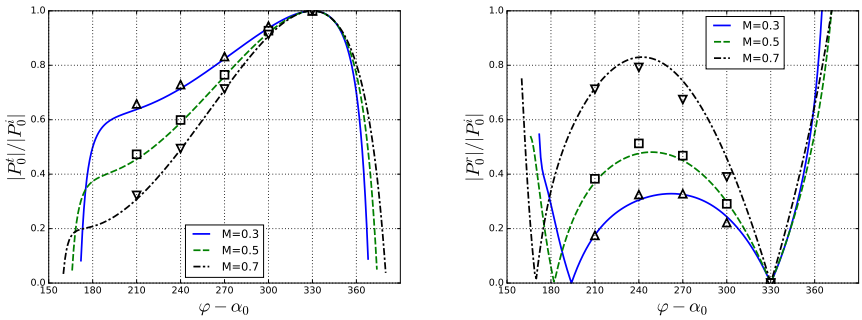

(a) $d = \cos\alpha_0 \approx 0.87$

(b) $d = \cos\alpha_0 \approx 0.87$

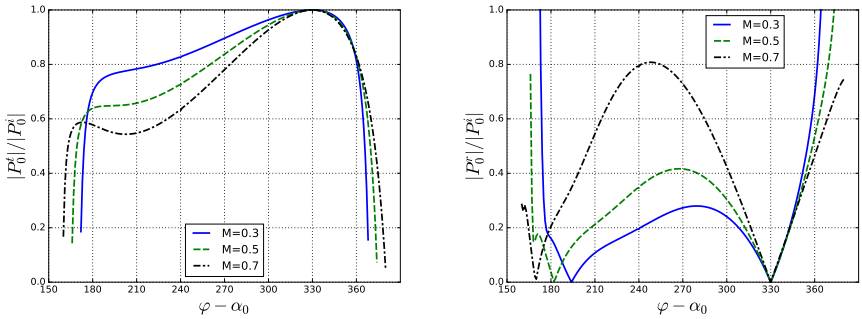

(c) $d = 2\cos\alpha_0 \approx 1.73$

(d) $d = 2\cos\alpha_0 \approx 1.73$

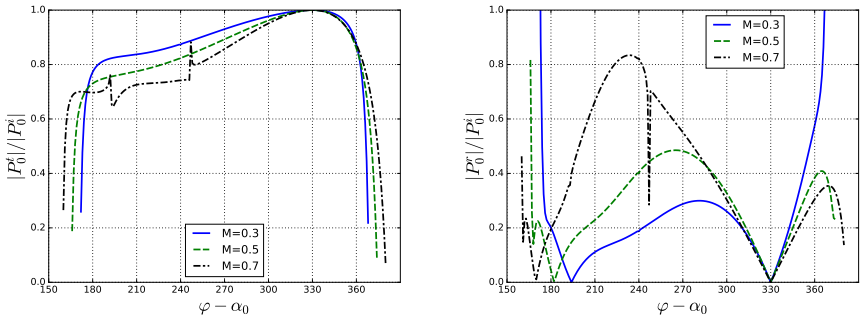

(e) $d = 3\cos\alpha_0 \approx 2.60$

(f) $d = 3\cos\alpha_0 \approx 2.60$

Figure 6: Relative transmission and reflection amplitudes of the incident wave. The points in figures 6a and 6b represent reference values taken from Koch [7].

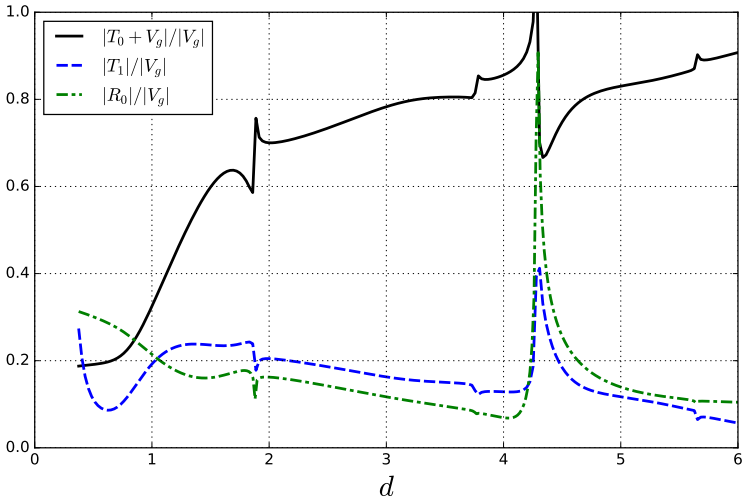

Figure 7: Relative transmission and reflection amplitudes as a function of d.

8. Concluding remarks

In this paper we have developed the first analytical solution to the scattering problem of a cascade of finite-length non-overlapping blades. The solution was achieved using the Wiener-Hopf method on a system of coupled scalar equations. This allowed us to express the scattered field only relying on the solution of an infinite algebraic system with decaying coefficients, which can be provably truncated to achieve convergent numerical approximations. In contrast, all previous work resulted in systems that are well-behaved when $d \leq 1$, but whose coefficients are exponentially increasing when $d > 1$, thus cannot yield a valid approximation in that case. Our solution applies in a general regime including effects of spanwise wavenumber and cross-flow, as well as incident acoustic and vortical waves, and we provided explicit expressions for the total unsteady lift on each blade as well as the far-field sound upstream and downstream of the cascade. We found that our solution applies to both the overlapping, $d < 1$, and the non-overlapping regime, $d \geq 1$, which showed that a number of features such as the form of the far-field is shared between the regimes, and that quantities such as the total lift transition smoothly as d increases across $d = 1$. We have also provided extensive numerical results demonstrating both the accuracy of our solution in comparison to previous work, and the type of predictions that we are able to achieve for the first time in the non-overlapping regime. This includes the study of transmission amplitudes as the gap spacing increases as well as the effect of the stagger angle α on the lift for large solidity.

A significant advantage of this exact solution is that its analytical nature will allow for the inclusion of additional features such as blade camber and thickness and for extensions to annular (periodic) geometries. These effects were

previously included based on exact solutions for the overlapping blade case, for instance by Posson et al. [14] and by Baddoo and Ayton [16], and we expect that this can be achieved also for the non-overlapping case in future research. A further assumption that could potentially be weakened is the zero angle of attack of the incident mean flow. Indeed Myers and Kerschen [22] provide an asymptotic analysis (for high frequencies and small incidence angles) which allows the study of such effects for single blades. Since the leading order term of their asymptotic expansion is simply the case of uniform mean-flow, we expect that it is possible to study these perturbations in a similar way for a cascade of blades.

9. Acknowledgements

The authors gratefully acknowledge support from the UK Engineering and Physical Sciences Research Council (EPSRC) grant EP/L016516/1 for the University of Cambridge Centre for Doctoral Training, the Cambridge Centre for Analysis.

Appendix A. The kernel κ and its factorisation

For completeness we provide a brief overview of the Wiener-Hopf factorisation of $\kappa(\alpha)$. This and very similar kernels have already been factorised by Koch [7], Peake [8] and Glegg [11], and the reader is referred to these papers for a detailed treatment. The kernel κ is meromorphic with simple poles at $k_n^{\pm}$ and zeros at $\tilde{\Omega}\frac{M}{M_x}, \sigma_m^{\pm}$ which cluster linearly along the following rays as $|m|, n \to \infty$:

$$\sigma_m^{\pm} \sim 2\pi \frac{-d \pm is\beta}{s^2\beta^2 + d^2} m + \frac{\mp isdMM_x\tilde{\Omega}/\beta \pm is\beta\sigma - MM_x\tilde{\Omega}s^2 - d\sigma}{s^2\beta^2 + d^2} \text{ as } m \to +\infty \tag{A.1}$$

$$\sigma_{-m}^{\pm} \sim 2\pi \frac{d \pm is\beta}{s^2\beta^2 + d^2} m + \frac{\pm isdMM_x\tilde{\Omega}/\beta \mp is\sigma\beta - MM_x\tilde{\Omega}s^2 - d\sigma}{s^2\beta^2 + d^2} \text{ as } m \to +\infty \tag{A.2}$$

$$k_n^{\pm} \sim \frac{\pm i\pi}{s\beta} n - \frac{MM_x\tilde{\Omega}}{\beta^2} \text{ as } n \to \infty.$$

Thus by the Weierstrass factorisation theorem (see theorem 5.14 in [20, p. 170] or the special case given in [19, p. 40]) we can express κ in the form

$$\kappa(\alpha) = e^{g(\alpha)}(1 - \alpha M_x/(\tilde{\Omega}M)) \frac{\prod_{m\in\mathbb{Z}} (1 - \alpha/\sigma_m^-)\, e^{\alpha/\sigma_m^-} \prod_{m\in\mathbb{Z}} (1 - \alpha/\sigma_m^+)\, e^{\alpha/\sigma_m^+}}{\prod_{n=0}^{\infty} \left(1 - \alpha/k_n^-\right) e^{\alpha/k_n^-} \prod_{n=0}^{\infty} \left(1 - \alpha/k_n^+\right) e^{\alpha/k_n^+}}$$

where $g(\alpha)$ is some entire function. This suggests a construction of κ^+ as follows

$$\kappa^+(\alpha) = e^{\chi_1(\alpha)}(1 - \alpha M_x/(\tilde{\Omega}M)) \frac{\left(1 - \alpha/\sigma_0^-\right)}{\left(1 - \alpha/k_0^-\right)} \prod_{n=1}^{\infty} \frac{(1 - \alpha/\sigma_n^-)\left(1 - \alpha/\sigma_{-n}^-\right)}{\left(1 - \alpha/k_n^-\right)}.$$

Let us denote $a_1 = 2\pi\frac{-d-is\beta}{s^2\beta^2+d^2}, a_2 = 2\pi\frac{d-is\beta}{s^2\beta^2+d^2}, a_3 = -\frac{i\pi}{s\beta}$, then the infinite products in above expression are well-defined because, for any fixed $\alpha \in R^+$, as $n \to \infty$ the factors have the asymptotic behaviour

$$\frac{\left(1-\alpha/\sigma_n^-\right)\left(1-\alpha/\sigma_{-n}^-\right)}{\left(1-\alpha/k_n^-\right)} \sim \frac{\left(1-\frac{\alpha}{a_1 n}+\mathcal{O}(n^{-2})\right)\left(1-\frac{\alpha}{a_2 n}+\mathcal{O}(n^{-2})\right)}{\left(1-\frac{\alpha}{a_3 n}+\mathcal{O}(n^{-2})\right)}$$
$$\sim 1-\frac{\alpha}{n}\underbrace{\left(\frac{1}{a_1}+\frac{1}{a_2}-\frac{1}{a_3}\right)}_{=0}+\mathcal{O}(n^{-2}) \sim 1+\mathcal{O}(n^{-2}).$$

To analyse the behaviour of κ^+ and find a suitable choice of χ_1, we can use the following result from Noble [19, p. 128]:

Lemma 1 (Consequence of Stirling's formula)**.** *Let*

$$F(\alpha) = \prod_{n=1}^{\infty}(1+\alpha/\alpha_n)e^{-\alpha/\beta_n}$$

and suppose that $\alpha_n = an+b+\mathcal{O}(n^{-1})$ and $\beta_n = an+c+\mathcal{O}(n^{-1})$ as $n \to \infty$. Then we have for any $\epsilon > 0$: As $\alpha \to \infty$ in $\operatorname{Im}\alpha > -\operatorname{Im}(\alpha_1)+\epsilon$, where α_1 is the root of $F(\alpha)$ with smallest imaginary part, that

$$F(\alpha) \sim C_1 \exp\left(\frac{\alpha}{a}(1-\gamma)-\left(\frac{\alpha}{a}+\frac{b}{a}+\frac{1}{2}\right)\ln\left(\frac{\alpha}{a}+\frac{b}{a}+1\right)+\alpha\sum_{n=1}^{\infty}\left(\frac{1}{an}-\frac{1}{\beta_n}\right)\right),$$

where γ is the Euler-Mascheroni constant.

Applying this lemma to our expression for κ^+ shows, after a few steps of algebra, that:

$$\kappa^+(\alpha) \sim \alpha^{\frac{1}{2}}\exp\left[\chi_1(\alpha)+\alpha\left(\frac{1}{a_1}\ln\left(\frac{a_3}{a_1}\right)+\frac{1}{a_2}\ln\left(\frac{a_3}{a_2}\right)\right)\right] \quad \text{as } \alpha \to \infty \text{ in } R^+.$$

Thus by choosing

$$\chi_1(\alpha) = -\alpha\left(\frac{1}{a_1}\ln\left(\frac{a_3}{a_1}\right)+\frac{1}{a_2}\ln\left(\frac{a_3}{a_2}\right)\right),$$

we can ensure that $\kappa^+(\alpha) \sim \alpha^{\frac{1}{2}}$ as $\alpha \to \infty$ in R^-. Using lemma 1 one finds $g(\alpha)$ to be a constant and so the equivalent expression for κ^- can easily be found from κ/κ^-, which behaves as $\kappa^-(\alpha) \sim \alpha^{-\frac{1}{2}}$ as $\alpha \to \infty$ in R^-.

Finally, we note that in this construction $\kappa^\pm$ are only defined up to a multiplicative constant, and thus in our numerical implementation we fix the factors by requiring that $\kappa^+(0) = \kappa(0)$.

Appendix B. Wiener-Hopf splitting for the trailing edge correction

We have outlined in §4.3 how to additively split the term

$$g(\alpha) = \frac{1}{\kappa^-(\alpha)} \left(\left[\tilde{P}_1^+ \right] (\alpha) + \left[\tilde{P}_3^+ \right] (\alpha) \right),$$

and in this appendix we provide the detailed derivation of this splitting. Firstly we recall from §4.1 that

$$\left[P_1^+ \right] (\alpha) \propto \frac{\kappa^+(\alpha)}{\alpha - \tilde{\sigma}_\eta^-}, \quad \eta = 0, 1.$$

Thus taking inverse and half-line transform we find:

$$\begin{aligned} \left[\tilde{P}_1^+ \right] (\alpha) &\propto e^{-i\alpha} \int_1^\infty \int_{-\infty}^\infty e^{-ix(\alpha'-\alpha)} \frac{1}{\alpha' - \alpha'} \frac{\kappa^+(\alpha')}{\alpha - \tilde{\sigma}_\eta^-} d\alpha' dx \\ &\propto e^{-i\alpha} \int_1^\infty \int_{\Gamma_-} e^{-ix(\alpha'-\alpha)} \frac{1}{\alpha' - \alpha} \frac{\kappa^+(\alpha')}{\alpha' - \tilde{\sigma}_\eta^-} d\alpha' dx \\ &\propto \int_{\Gamma_-} e^{-i\alpha'} \frac{1}{\alpha' - \alpha} \frac{\kappa^+(\alpha')}{\alpha' - \tilde{\sigma}_\eta^-} d\alpha', \end{aligned} \tag{B.1}$$

where in the second line we use the properties of κ^+ established in §4.2 to change the contour of integration to Γ^- which at its tails behaves like $\arg \alpha \sim -\tilde{\epsilon}\,\mathrm{sign}(\mathrm{Re}\,\alpha), 0 < \tilde{\epsilon} \ll 1$. It is possible to change to this contour since we observed in §4.2 that κ^+ is analytic and of algebraic behaviour in the domain

$$\begin{aligned} \mathcal{D} = R^+ \cup \Bigg\{ \alpha \Big| \arg \alpha \in \Bigg(&- \arctan\left(\frac{s\beta}{d} \right), \arctan\left(\frac{s\beta}{d} \right) \Bigg) \\ &\cup \left(\pi - \arctan\left(\frac{s\beta}{d} \right), \pi + \arctan\left(\frac{s\beta}{d} \right) \right) \Bigg\}, \end{aligned}$$

which in particular contains Γ^- (see figure B.8). Along this contour the integrand is integrable in the product space and so Fubini's theorem applies, and we can exchange order of integration as we did in the third line.

We note now that the final integral in Eq. (B.1) has integrand with exponential decay along Γ_- and thus there is a constant C such that for all $\alpha \in R^+$:

$$\left| \left[\tilde{P}_1^+ \right] (\alpha) \right| \leq C|\alpha|^{-1} \int_{\Gamma_-} \left| e^{-i\alpha'} \frac{\kappa^+(\alpha')}{\alpha' - \Omega} \right| d\alpha', \quad \text{i.e.} \quad \left[\tilde{P}_1^+ \right] (\alpha) = \mathcal{O}\left(\alpha^{-1} \right).$$

As mentioned in §4.3, imposing the unsteady Kutta condition at the trailing edge implies that the pressure field must be non-singular at $x = 1$ (see for instance [8], p. 274), which means that the above behaviour of $\left[\tilde{P}_1^+ \right] (\alpha)$ is indeed expected. Imposing the unsteady Kutta condition (condition (vi) in §2.1) at the trailing edge to $[p_2]$ and noting that $[p_3](x) = -[p_1](x) - [p_2](x)$, for $x > 1$, we conclude that the pressure jump $[p_3](x)$ must be non-singular at $x = 1$, and it can thus

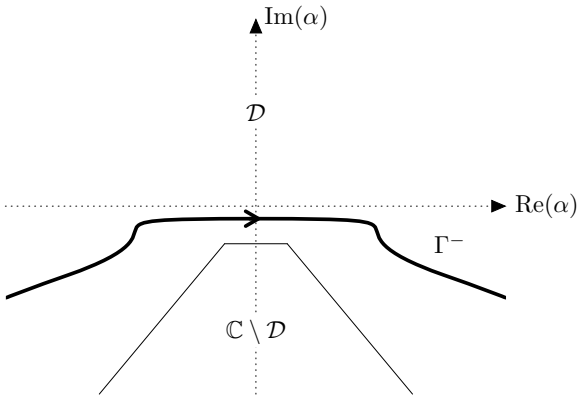

Figure B.8: The domain $\mathcal{D}$ of algebraic behaviour of $|\kappa^+|$ in the complex α-plane.

be shown by integration-by-parts that $\left[\tilde{P}_3^+\right](\alpha) = \mathcal{O}\left(\alpha^{-1}\right)$ as $\alpha \to \infty, \alpha \in R^+$. As noted in §4.3 this implies that there is a strip $\mathcal{S}$ containing the real axis and a constant C such that

$$|g(\alpha)| \leq C\left(1 + |\operatorname{Re}\alpha|\right)^{-\frac{1}{2}}, \text{ for all } \alpha \in \mathcal{S},$$

which allows us to apply theorem B from [19, p. 13]. This yields the additive splitting $g = g_- + g_+$ where:

$$g_+(\alpha) = \frac{1}{2\pi i}\int_{-\infty-ic}^{\infty-ic} \frac{g(\zeta)}{\zeta-\alpha}d\zeta \text{ and } g_-(\alpha) = \frac{1}{2\pi i}\int_{-\infty+ic}^{\infty+ic} \frac{g(\zeta)}{\zeta-\alpha}d\zeta.$$

These functions are analytic in R^+ and R^- respectively (after shrinking the domains $R^\pm$ if necessary), and they are bounded in their respective half-planes, since: For all α, with $\operatorname{Im}\alpha > -\delta$,

$$\left|\int_{-\infty-ic}^{\infty-ic} \frac{g(\zeta)}{\zeta-\alpha}d\zeta\right| \leq C\int_{-\infty}^{\infty} \frac{(1+|t|)^{-\frac{1}{2}}}{|t-ic-\alpha|}dt \leq \sqrt{2}C\int_{-\infty}^{\infty} \frac{(1+|t|)^{-\frac{1}{2}}}{|t-\operatorname{Re}\alpha|+|c-\delta|}dt,$$

and so the boundedness of g_+ in R^+ is a consequence of the following lemma:

Lemma 2. *Let $\epsilon > 0$, then the function $I : \mathbb{R} \to \mathbb{R}$, defined by*

$$I(y) := \int_{-\infty}^{\infty} \frac{(1+|t|)^{-\frac{1}{2}}}{|t-y|+\epsilon}dt,$$

is bounded.

Proof. For $y \neq 0$:

$$\begin{aligned} I'(y) &= \int_{-\infty}^{\infty} \frac{-\operatorname{sign}(t-y)(1+|t|)^{-\frac{1}{2}}}{(|t-y|+\epsilon)^2} dt \\ &= \int_{-\infty}^{y} \frac{(1+|t|)^{-\frac{1}{2}}}{(|t-y|+\epsilon)^2} dt - \int_{y}^{\infty} \frac{(1+|t|)^{-\frac{1}{2}}}{(|t-y|+\epsilon)^2} dt \\ &= \int_{-\infty}^{0} \frac{(1+|t-y|)^{-\frac{1}{2}}}{(|t|+\epsilon)^2} dt - \int_{0}^{\infty} \frac{(1+|t-y|)^{-\frac{1}{2}}}{(|t|+\epsilon)^2} dt \begin{cases} \leq 0, & \text{if } y > 0 \\ \geq 0, & \text{if } y < 0. \end{cases} \end{aligned}$$

□

The boundedness of g_- in R^- follows analogously. This allows us to solve the trailing-edge correction problem as shown in Eq. (27).

Appendix C. Reduction to an infinite algebraic system

In §5 we outlined how the scattering problem can be reduced to the solution of an infinite algebraic system, by repeated application of Fourier inversion and change of order of integration. Here we justify these steps rigorously: To derive Eq. (30) note that

$$\begin{aligned} \left[P_2^-\right](\alpha') &= \frac{1}{2\pi} \int_{-\infty}^{0} \int_{-\infty}^{\infty} e^{ix(\alpha'-\alpha)} e^{i\alpha} \left[\tilde{P}_2^-\right](\alpha) d\alpha dx \\ &= \frac{1}{2\pi} \int_{-\infty}^{0} \int_{-\infty+i\epsilon}^{\infty+i\epsilon} e^{ix(\alpha'-\alpha)} e^{i\alpha} \left[\tilde{P}_2^-\right](\alpha) d\alpha dx \\ &= \frac{-1}{2\pi i} \int_{-\infty+i\epsilon}^{\infty+i\epsilon} \frac{1}{\alpha-\alpha'} e^{i\alpha} \kappa^-(\alpha) \\ &\qquad \sum_{m\in\mathbb{Z}} \frac{1}{\alpha-\tilde{\sigma}_m^+} \operatorname{Res}\left(\frac{1}{\kappa^-}, \tilde{\sigma}_m^+\right) \left(\left[\tilde{P}_1^+\right](\tilde{\sigma}_m^+) + \left[\tilde{P}_3^+\right](\tilde{\sigma}_m^+)\right) d\alpha, \end{aligned}$$

where in the second line we changed the contour for some small $\epsilon > 0$ (small enough to remain within $R^+ \cap R^-$) using Cauchy's theorem and the analyticity of the integrand, and in the third line we used absolute integrability in the product space (along the given contours) to exchange the order of integration by Fubini's theorem, and we substituted $\left[\tilde{P}_2^-\right](\alpha)$ using Eq. (27). Using the linear asymptotic growth of $\tilde{\sigma}_m^+$ (cf. Eq. (A.1),(A.2)), and the form of residues from Eq. (21), we observe that

$$\sum_{m\in\mathbb{Z}} \left| \frac{1}{\alpha-\tilde{\sigma}_m^+} \operatorname{Res}\left(\frac{1}{\kappa^-}, \tilde{\sigma}_m^+\right) \left(\left[\tilde{P}_1^+\right](\tilde{\sigma}_m^+) + \left[\tilde{P}_3^+\right](\tilde{\sigma}_m^+)\right) \right|$$

is uniformly bounded for $\mathrm{Im}(\alpha) = \epsilon$. Thus we have sufficient decay, of order $O\left(\alpha^{-\frac{3}{2}}\right)$, for

$$\left|\frac{1}{\alpha-\beta}e^{i\alpha}\kappa^-(\alpha)\right|\sum_{m\in\mathbb{Z}}\left|\frac{1}{\alpha-\tilde{\sigma}_m^+}\,\mathrm{Res}\left(\frac{1}{\kappa^-},\tilde{\sigma}_m^+\right)\left(\left[\tilde{P}_1^+\right](\tilde{\sigma}_m^+)+\left[\tilde{P}_3^+\right](\tilde{\sigma}_m^+)\right)\right|$$

to be integrable along the given contour. Therefore the dominated convergence theorem applies and we can exchange order of summation and integration to find

$$\begin{aligned}\left[P_2^-\right](\alpha') = \sum_{m\in\mathbb{Z}}\Bigg[&\left(\left[\tilde{P}_1^+\right](\tilde{\sigma}_m^+)+\left[\tilde{P}_3^+\right](\tilde{\sigma}_m^+)\right)\\ &\frac{(-1)}{2\pi i}\int_{-\infty+i\epsilon}^{\infty+i\epsilon}\frac{1}{\alpha-\alpha'}e^{i\alpha}\kappa^-(\alpha)\frac{1}{\alpha-\tilde{\sigma}_m^+}\,\mathrm{Res}\left(\frac{1}{\kappa^-},\tilde{\sigma}_m^+\right)d\alpha\Bigg].\end{aligned}$$

Thus noting that $B_j = \left[P_2^-\right](\tilde{\sigma}_m^-)$ this yields precisely Eq. (30). Similarly by considering Eq. (28) we find

$$\begin{aligned}\left[\tilde{P}_3^+\right](\alpha') &= \frac{1}{2\pi}e^{-i\alpha'}\int_1^\infty\int_{-\infty}^{\infty}e^{ix(\alpha'-\alpha)}\left[P_3^+\right](\alpha)d\alpha dx\\ &= \frac{1}{2\pi}e^{-i\alpha'}\int_1^\infty\int_{-\infty-i\epsilon}^{\infty-i\epsilon}e^{ix(\alpha'-\alpha)}\left[P_3^+\right](\alpha)d\alpha dx\\ &= -\frac{1}{2i\pi}\int_{-\infty-i\epsilon}^{\infty-i\epsilon}\frac{1}{\alpha'-\alpha}e^{-i\alpha}\left[P_3^+\right](\alpha)d\alpha\\ &= -\frac{1}{2i\pi}\int_{-\infty-i\epsilon}^{\infty-i\epsilon}\frac{1}{\alpha'-\alpha}e^{-i\alpha}\kappa^+(\alpha)\\ &\qquad\sum_{m\in\mathbb{Z}}\frac{1}{\alpha-\tilde{\sigma}_m^-}\,\mathrm{Res}\left(\frac{1}{\kappa^+},\tilde{\sigma}_m^-\right)\left[P_2^-\right](\tilde{\sigma}_m^-)d\alpha.\end{aligned}$$

Here we cannot interchange the integration and summation straight away since $|\kappa^+|$ grows like $|\alpha|^{\frac{1}{2}}$ along this contour. We note, however, that the sum is again uniformly bounded along the given contour and remains so if we change to a contour Γ^-, which at its tails behaves like $\arg\alpha \sim -\tilde{\epsilon}\,\mathrm{sign}(\mathrm{Re}\,\alpha), 0 < \tilde{\epsilon} \ll 1$. This change of contour is analogous to the one applied in Appendix B. Along Γ^- we observe exponential decay of the integrand, so absolute convergence on the product space for sum and integrand, so we can exchange the order of summation and integration to find Eq. (31).

Appendix D. The finite section method and convergence

Here we provide a more detailed description of the finite section method which we apply to approximately solve Eq. (33). We also include a brief proof of convergence for this method when it is applied to our linear system.

Working on $l^2(\mathbb{Z})$ we shall denote by $P_m \in \mathcal{B}(l^2(\mathbb{Z}))$ the projection onto the coordinates $-m, -m+1, \ldots, m-1, m$ and we implicitly identify $P_m(l^2(\mathbb{Z})) \cong \mathbb{C}^{2m+1}$. We employ the following version of the finite section method which is described and analysed by [23]: Our approximation of the solution to the system $Lx = b$ is $\Gamma_m(L, b)$ defined by

$$\Gamma_m(L,b) = \begin{cases} (0)_{j\in\mathbb{Z}}, \text{ if } \min\{\text{singular values of } P_m L^* P_{m+1} L P_m\} \leq \frac{1}{m} \\ (P_m L^* P_{m+1} L P_m)^{-1} P_m L^* P_{m+1} b, \text{ otherwise,} \end{cases} \tag{D.1}$$

which essentially corresponds to truncating the normal equations $L^*Lx = L^*b$ to $2m+1$ entries and solving the resulting system on $\mathbb{C}^{2m+1}$.

Below we will show that, provided $(I - \mathbf{GF})$ is invertible, $\Gamma_m(I - \mathbf{GF}, A)$ converges to the true solution B as $m \to \infty$. Given the decay in the entries of $\mathbf{F}$ as shown in Eq. (D.2) we also have $P_m \mathbf{F} P_m B \to C$ as $m \to \infty$. Thus all of these facts combined mean that the finite section method can be applied to our algebraic system Eq. (33)-(34) and provides a valid way to approximately solve the scattering problem.

In order to prove that $\Gamma_m(I - \mathbf{GF}, A)$ converges to the true solution B as $m \to \infty$ we introduce the following notation: We write $A(x) \lesssim B(x)$, for functions $A(x), B(x)$, when there exists a constant $\mathcal{K} > 0$ independent of x such that $A(x) \leq \mathcal{K} B(x)$. To begin with let us look more closely at the coefficients in the linear system: Considering Eq. (32) we firstly note that the $e^{-i\alpha}$ term in the integrand decays exponentially along the given contour, thus we can estimate:

$$\begin{aligned} |\mathbf{F}_{jm}| &\lesssim \int_{\Gamma^-} \left|e^{-i\alpha}\kappa^+(\alpha)\right| \left|\frac{1}{\alpha - \tilde{\sigma}_j^+} \frac{1}{\alpha - \tilde{\sigma}_m^-}\right| d\alpha \left|\operatorname{Res}\left(\frac{1}{\kappa^+}, \tilde{\sigma}_m^-\right)\right| \\ &\lesssim \int_{\Gamma^-} \left|e^{-i\alpha}\kappa^+(\alpha)\right| d\alpha j^{-1} m^{-\frac{3}{2}} \lesssim j^{-1} m^{-\frac{3}{2}}, \end{aligned} \tag{D.2}$$

for some constant that does not depend on j, m. In the above derivation we also used the growth of the residues of $\frac{1}{\kappa^+}$ as we established in §4.2. We can change the contour of integration for $\mathbf{G}_{jm}$ to one that is of V shape with tails of the form $\arg\alpha \sim \tilde{\epsilon}\operatorname{sign}(\operatorname{Re}\alpha), 0 < \tilde{\epsilon} \ll 1$. This way we ensure the same exponential decay of the integrand and we can similarly deduce

$$|\mathbf{G}_{jm}| \lesssim j^{-1} m^{-\frac{1}{2}}. \tag{D.3}$$

Eq. (D.2)-(D.3) allow us to show that $\mathbf{GF}$ is a well-defined bounded linear

operator on $l^2(\mathbb{Z})$, since it is clearly linear, and for $x \in l^2(\mathbb{Z})$:

$$\begin{aligned}\|\mathbf{GF}x\|_2^2 &= \sum_{l\in\mathbb{Z}} \left| \sum_{m\in\mathbb{Z}} \mathbf{G}_{lm} \sum_{j\in\mathbb{Z}} \mathbf{F}_{mj} x_j \right|^2 \\ &\lesssim \sum_{l\in\mathbb{Z}} \left[\sum_{m\in\mathbb{Z}} (1+|l|)^{-1}(1+|m|)^{-\frac{1}{2}} \sum_{j\in\mathbb{Z}} (1+|m|)^{-1}(1+|j|)^{-\frac{3}{2}} |x_j| \right]^2 \\ &\lesssim \sum_{l\in\mathbb{Z}} (1+|l|)^{-2} \left[\sum_{m\in\mathbb{Z}} (1+|m|)^{-\frac{3}{2}} \left(\sum_{j\in\mathbb{Z}} (1+|j|)^{-3} \right)^{\frac{1}{2}} \|x\|_2 \right]^2 \lesssim \|x\|_2^2,\end{aligned}$$

where the constants in the above estimates are independent of x. Assuming that $L = I - \mathbf{GF}$ is in fact invertible the following condition (proved in [23], p. 60) is sufficient to ensure $\Gamma_m(L, b)$ as defined in Eq. (D.1) converges to $L^{-1}b$ in $l^2(\mathbb{Z})$:

$$\max\left\{\|(I-P_{m+1})LP_m\|, \|P_mL(I-P_{m+1})\|\right\} \to 0 \text{ as } m \to \infty. \tag{D.4}$$

Claim 1. *The condition Eq.* (D.4) *is satisfied for* $L = I - \mathbf{GF}$.

Proof. Write $\mathbf{H} = \mathbf{GF}$. We aim to show that

$$\max\left\{\|(I-P_{m+1})(I-\mathbf{H})P_m\|, \|P_m(I-\mathbf{H})(I-P_{m+1})\|\right\} \to 0 \text{ as } m \to \infty.$$

Note that

$$(I-P_{m+1})IP_m = 0,$$

thus it is sufficient to prove the above estimate for $\mathbf{H}$ directly. Now we have for an arbitrary $x \in l^2(\mathbb{Z})$:

$$\begin{aligned}\|(I-P_{m+1})\mathbf{H}P_mx\|_2^2 &\le \sum_{|i|>m+1} \left(\sum_{|j|<m} |\mathbf{H}_{kj}x_j| \right)^2 \\ &\le \sum_{|k|>m+1} \sum_{|j|<m} |\mathbf{H}_{kj}|^2 \|x\|^2 \\ &\lesssim \|x\|^2 \sum_{|k|>m+1} \sum_{|j|<m} (1+|k|)^{-2}(1+|j|)^{-3} \\ &\lesssim \|x\|^2 \sum_{|k|>m+1} (1+|k|)^{-2} \sum_{j\in\mathbb{Z}} (1+|j|)^{-3} \\ &\lesssim \|x\|^2 \sum_{|k|>m+1} (1+|k|)^{-2} \to 0 \text{ as } m \to \infty.\end{aligned}$$

Similarly

$$\begin{aligned}\|P_m\mathbf{H}(I-P_{m+1})x\|_2^2 &\lesssim \|x\|^2 \sum_{|k|<m}\sum_{|j|>m+1}(1+|k|)^{-2}(1+|j|)^{-3}\\ &\lesssim \|x\|^2 \sum_{|j|>m+1}(1+|j|)^{-3} \to 0 \text{ as } m\to\infty.\end{aligned}$$

□

Therefore, provided $I-\mathbf{GF}$ is invertible, we have indeed

$$\Gamma_m\left(I-\mathbf{GF},A\right) \xrightarrow{l^2} \left(I-\mathbf{GF}\right)^{-1}A \text{ as } m\to\infty.$$

References

[1] N. Peake, A. B. Parry, Modern challenges facing turbomachinery aeroacoustics, Annual Review of Fluid Mechanics 44 (1) (2012) 227–248.

[2] J. Carlson, A. Heins, The reflection of an electromagnetic plane wave by an infinite set of plates, I, Quarterly of Applied Mathematics 4 (4) (1947) 313–329.

[3] A. E. Heins, J. Carlson, The reflection of an electromagnetic plane wave by an infinite set of plates, II, Quarterly of Applied Mathematics 5 (1) (1947) 82–88.

[4] A. E. Heins, The reflection of an electromagnetic plane wave by an infinite set of plates, III, Quarterly of Applied Mathematics 8 (3) (1950) 281–291.

[5] S. Kaji, T. Okazaki, Propagation of sound waves through a blade row: II. Analysis based on the acceleration potential method, Journal of Sound and Vibration 11 (3) (1970) 355–375.

[6] D. S. Whitehead, Vibration and Sound Generation in a Cascade of Flat Plates in Subsonic Flow, University of Cambridge Department of Engineering Reports and Memoranda No. 3685, 1970.

[7] W. Koch, On the transmission of sound waves through a blade row, Journal of Sound and Vibration 18 (1) (1971) 111–128.

[8] N. Peake, The interaction between a high-frequency gust and a blade row, Journal of Fluid Mechanics 241 (1992) 261–289.

[9] N. Peake, E. J. Kerschen, A uniform asymptotic approximation for high-frequency unsteady cascade flow, Proc. R. Soc. Lond. A 449 (1935) (1995) 177–186.

[10] N. Peake, The scattering of vorticity waves by an infinite cascade of flat plates in subsonic flow, Wave Motion 18 (3) (1993) 255–271.

[11] S. Glegg, The response of a swept blade row to a three-dimensional gust, Journal of Sound and Vibration 227 (1) (1999) 29–64.

[12] N. Peake, E. J. Kerschen, Influence of mean loading on noise generated by the interaction of gusts with a flat-plate cascade: upstream radiation, Journal of Fluid Mechanics 347 (1997) 315–346.

[13] N. Peake, E. J. Kerschen, Influence of mean loading on noise generated by the interaction of gusts with a cascade: downstream radiation, Journal of Fluid Mechanics 515 (2004) 99–133.

[14] H. Posson, S. Moreau, M. Roger, On the use of a uniformly valid analytical cascade response function for fan broadband noise predictions, Journal of Sound and Vibration 329 (18) (2010) 3721–3743.

[15] L. J. Ayton, N. Peake, On high-frequency noise scattering by aerofoils in flow, Journal of Fluid Mechanics 734 (2013) 144–182.

[16] P. J. Baddoo, L. J. Ayton, An analytic solution for gust–cascade interaction noise including effects of realistic aerofoil geometry, Journal of Fluid Mechanics 886 (2020) A1.

[17] M. E. Goldstein, Aeroacoustics, McGraw-Hill, New York, 1976.

[18] D. G. Crighton, The Kutta Condition in Unsteady Flow, Annual Review of Fluid Mechanics 17 (1) (1985) 411–445.

[19] B. Noble, Methods based on the Wiener-Hopf Technique for the Solution of Partial Differential Equations, Pergamon Press, London, 1958.

[20] J. B. Conway, Functions of One Complex Variable I, Springer, New York, 1978.

[21] R. Mani, G. Horvay, Sound transmission through blade rows, Journal of Sound and Vibration 12 (1) (1970) 59–83.

[22] M. R. Myers, E. J. Kerschen, Influence of incidence angle on sound generation by airfoils interacting with high-frequency gusts, Journal of Fluid Mechanics 292 (1995) 271–304.

[23] J. Ben-Artzi, A. C. Hansen, O. Nevanlinna, M. Seidel, Can everything be computed? - On the Solvability Complexity Index and Towers of Algorithms, arXiv preprint, arXiv:1508.03280v1 (2015).